Summer 2004

The Paleomagnetism of the Stewart's Point and Anchor Bay Members of the Point Arena Terrane, Northern California

Kirk Heim
Western Washington University

Paleomagnetism of the Stewart's Point and Anchor Bay members of the Point Arena terrane, northern California

by

Kirk Allen Heim

Accepted in partial completion

Of the Requirements for the Degree

Master of Science

Moheb A. Ghali, Dean of the Graduate School

ADVISORY COMMITTEE

Chair, Dr. Bernard A. Housen

Dr. Russ F. Burmester

Dr. Juliet Crider

The paleomagnetism of the Stewart's Point and Anchor Bay members of the Point Arena terrane, northern California

A Thesis
Presented to
The faculty of
Western Washington University

In Partial Fulfillment
Of the Requirements for the Degree
Master of Science

By
Kirk Heim
June 2004

MASTER'S THESIS

In presenting this thesis in partial fulfillment of the requirements for a master's degree at Western Washington University, I grant to Western Washington University the non-exclusive royalty-free right to archive, reproduce, distribute, and display the thesis in any and all forms, including electronic format, via any digital library mechanisms maintained by WWU.

I represent and warrant this is my original work and does not infringe or violate any rights of others. I warrant that I have obtained written permissions from the owner of any third party copyrighted material included in these files.

I acknowledge that I retain ownership rights to the copyright of this work, including but not limited to the right to use all or part of this work in future works, such as articles or books.

Library users are granted permission for individual, research and non-commercial reproduction of this work for educational purposes only. Any further digital posting of this document requires specific permission from the author.

Any copying or publication of this thesis for commercial purposes, or for financial gain, is not allowed without my written permission.

Name: Kirk Heim

Signature: _____

Date: 6/7/2018

MASTER'S THESIS

In presenting this thesis project in partial fulfillment of the requirements for a master's degree at Western Washington University, I agree that the Library shall make its copies freely available for inspection. I further agree that copying of this thesis project in whole or in part is allowable only for scholarly purposes. It is understood, however, that any copying or publication of this thesis for commercial purposes, or for financial gain, shall not be allowed without my written permission.

Signature _____

Date 8/6/2004

ABSTRACT

Paleomagnetic investigation of Upper Cretaceous sedimentary strata of the Point Arena terrane has shown the rocks to be remagnetized. The study was initially intended to reconstruct the Cretaceous paleogeography of the Point Arena terrane and resolve conflicting translation estimates, but became one of remagnetization. Samples studied are from the Upper Cretaceous Stewart's Point member and the Late Cretaceous Anchor Bay Member of the Gualala formation. Specimens surviving the remagnetization have a mean second-removed direction that indicates approximately 20 degrees vertical rotation from the expected direction of the Cretaceous magnetic field at the locality of the Point Arena terrane. The loss of original magnetization is most likely the result of a ChRM (chemical remanent magnetization) caused by orogenic fluid circulation. Reheating as the remagnetization mechanism can be ruled out by total lack of metamorphism. The paleomagnetic results of this study confirm a complex tectonic history for the Point Arena terrane. Once the nature and timing of the remagnetization events are better understood a more complete tectonic history can be determined.

ACKNOWLEDGMENTS

Dr. Russ Burmester has been invaluable in the laboratory and analysis phases of this project and has been a tremendous source of information. This manuscript has been greatly improved by his suggestions. I am indebted to Dr. Bernard Housen for his direction, assistance in the field, support and constructive criticism during this project. I want to thank Dr. Juliet Crider for her thorough review of this manuscript and suggestions for its presentation.

Carl Wentworth, Dave Engebretson and Clark Blake provided valuable information and insights. Katherine Kelleher created the base maps for this project and provided immeasurable support. Thanks to Basil Tikoff, Tammy Fawcett, and Allison Dean for support in the field. None of this could have happened without Chris Sutton and Vicki Critchlow. And thanks to ya'll up in the lab.

TABLE OF CONTENTS

TABLE OF FIGURES

TABLES

Introduction

Part of the western margin of North America has grown by the accretion of many terranes that were formed independently and added to North America during the Mesozoic and Cenozoic (Coney et al., 1980; Figure 1). One aspect of the geologic history of North America that has been under debate is the amount of post mid-Cretaceous latitudinal displacement of the coastal terranes located from Baja California to British Columbia, Canada.

Studies successful in determining primary paleomagnetic inclinations and therefore paleolatitudes from Cretaceous rocks of many of these terranes indicate various amounts of translation. Large (up to 3000 km) transport is estimated for the Insular Superterrane since 90 Ma (Beck and Noson, 1972; Wynne et al., 1995; Housen et al., 2003; Ward et al., 1997; Enkin et al., 2001). This translation is explained by the 'Baja BC' hypothesis (Irving, 1985), which proposes the original latitude of many of the West Coast terranes to be near that of present-day Baja California. Alternative reconstruction methods, based upon correlations of geologic units, have shown less than 1000 km offset for these same rocks (Monger and Price, 1996; Butler et al., 2001a).

A similar discrepancy exists between estimates of post-Cretaceous translation of terranes of coastal and Baja California (Dickinson and Butler, 1998; Schott et al., 2004; Kodama and Ward, 2001; Kanter, 1983; Kanter and Debiche, 1985; Champion et al., 1984). The initial goal of this paleomagnetic study of the Gualala Formation of the Point Arena terrane was to test the following possible paleogeographic models (Figure 2):

1. Dickinson and Butler's (1998) tectonic reconstruction model based on San Andreas fault offset indicating that the Point Arena terrane was

translated northward 575 km (5 degrees of paleolatitude). Geologic reconstructions based on provenance studies, most recently by Schott et al. (2004), indicating the amount of translation is ~450-650km, which is in agreement with fault-offset estimates.

2. A model by Kodama and Ward (2001) based on the paleontologic constraints of the paleoclimate zonation of habitats of the mollucan rudist, *Coralliochama orcutti*. The presence of the rudist in the Anchor Bay member of the Gualala Formation indicates a minimum of 1500 km post-Late Cretaceous offset by their model. A large displacement of approximately 1300km was derived by Kanter (1983), Kanter and Debiche (1985), and Champion et al. (1984) based on paleomagnetic results from the Eocene German Rancho Formation, which overlies the Gualala Formation in the Point Arena terrane. They obtained a paleolatitude of 25° N for these rocks, indicating 1300 km of post-Eocene northward translation. Addis (2003) studied the same units, but was unable to duplicate the results of Kanter (1983) and Kanter and Debiche (1985).

There has been no previous paleomagnetic study of the Anchor Bay member and Stewart's Point member of the Gualala Formation. The sediments of these units are good candidates for a paleomagnetic study because they are layered, which can be used to determine paleohorizontal, are folded, which can be used to test the age of magnetization versus deformation, and the ages of these units have been fairly well constrained. Furthermore, paleomagnetic results from the overlying Oligocene Iverson Basalt (Kanter, 1983) suggest that useful results can be obtained from the Point Arena terrane.

However, I show later that remanence postdates deformation so the values of beding and of depositional age are lost. Therefore, the intended comparison with the above models can not be completed. Instead, the results of this study were compared with results of other paleomagnetic studies of Upper Cretaceous sediments along the western margin of North America that indicate pervasive regional remagnetization.

Remagnetizations produced by orogenic fluids (i.e., connate brines) have been well-documented in carbonate rocks associated with the Allegheny (McCabe and Channel, 1994) and Laramide (Muttoni et al., 2001) fold and thrust belts. McCabe and Channel (1994) studied carbonates of the Craven Basin in England and concluded a remagnetization of the 'Appalachian' type had occurred. Directions from the Muttoni et al. (2001) study of Laramide deformation agree with Cretaceous North American cratonic reference directions and the exclusive occurrence of normal polarity suggests remagnetization occurred during the Cretaceous normal superchron.

An extensive paleomagnetic study of sedimentary and igneous rocks, mostly of Jura-Cretaceous age, from the terranes of the San Juan Islands, WA (Burmester et al., 2000) found that all units of that area that were affected by a Cretaceous high-P, low-T (prehnite facies) metamorphic event (see Brandon et al., 1988) were remagnetized following folding, confirming a prior study by Bogue et al. (1989). Other San Juan Island units such as the Haro Formation, unaffected by this metamorphism, also were remagnetized (Hults and Housen, 2000).

A paleomagnetic study of Cretaceous and Tertiary sedimentary rocks of the Klamath Mountains province of California found that the Cretaceous rocks have directions similar to younger geomagnetic field directions (Mankinen, 1982). The

paleomagnetic data pass a fold test with the mean direction approximating the Late Cretaceous direction, similar to that of the remagnetized Great Valley sequence. Mechanisms of remagnetization were not discussed by Mankinen.

A paleomagnetic study of Upper Jurassic and Lower Cretaceous Great Valley Group sediments from northern California and southwest Oregon (Frei and Blake, 1987) indicates a pervasive Late Cretaceous or Tertiary remagnetization was recorded by these rocks. The magnetizations were deemed secondary after failing a fold test, and are attributed to deep subaerial weathering, burial and uplift, or low-temperature chemical alteration.

Paleomagnetic data for Middle Jurassic pillow lavas and diabase sills of the Coast Range ophiolite at Mount Diablo, California, also indicate a remagnetization with a direction similar to that of the Late Cretaceous through late Cenozoic dipole field for North America (Hagstrum and Jones, 1998). The units studied have a positive reversal test, but no fold test was available to constrain the timing of the event. Because the Coast Range ophiolite at this locale was part of the overriding plate and not subjected to low-temperature, high-pressure alteration, the overprint is inferred to be Miocene or younger and may have been acquired during emplacement and seafloor alteration near a spreading ridge (Hagstrum and Jones, 1998).

These studies show there is a record of remagnetization of Upper Cretaceous sediments from the North American Cordillera. The process(es) that caused this remagnetization are important components of the tectonic history of the West Coast.

Geology and Structure of the Anchor Bay and Stewart's Point members

Geology

The Point Arena terrane is located on the northern California coast outboard of the San Andreas fault and includes the northernmost exposure of rocks west of the San Andreas fault (Figure 3). The Gualala Formation of the Point Arena terrane is composed of the Upper Cretaceous or Paleocene Anchor Bay member and the Upper Cretaceous Stewart's Point member (Figure 4). These two members contain conglomerates, sandstones and mudstones that are interpreted to be inner-, middle-, and outer-fan turbidite deposits (Wentworth, 1966). These are exposed along a 65 km stretch of sea cliffs in northern California, nearly 150 km north of San Francisco (Figure 5).

The Stewart's Point and Anchor Bay units are members of the Gualala Formation. Originally called the 'Wallowa' beds, The Gualala Formation was first described by Charles White (1885). Weaver (1944) separated the Gualala sedimentary rocks and basalt into distinct units. In 1966 Wentworth completed the most extensive geologic work of the area up to that time, which was published as his doctoral dissertation. Wentworth (1966) was able to say that the Gualala units were distinct from the Franciscan due to the absence of Franciscan clasts within any of the conglomerates of the Point Arena terrane's sedimentary rocks.

The Late Campanian Stewart's Point member is the lower sedimentary unit in the Gualala Formation. Age was determined by identification of ammonite fragments and foraminifers (Wentworth, 1966). A low-angle detachment fault forms the lower boundary with the basalt spilites of Black Point (Figure 6). The sediments range from fine-

grained to conglomerate. The sandstone of the Stewart's Point member is gray on fresh surface, fine- to medium-grained arkose and consists of 50% quartz with mixed K-feldspar and plagioclase. The conglomerate contains clasts composed of porphyritic volcanics and fine-grained granitic rocks. The exposed Stewart's Point sections are 1100 to 1400 meters thick.

Conformably overlying the Stewart's Point member is the Anchor Bay member (Figure 7). The Anchor Bay member has been determined to be Campanian-Mastrichtian based on the presence of *Coralliochama orcutti,* ammonite fragments and Tethyan foraminifera (Durham and Kirk, 1950; McDougall, 1998). Wentworth et al. (1998) and Mcdougall (1998) indicated the possibility of mixing of sediments in the upper portions of the Anchor Bay member with sediments that contained Paleocene foraminifers and Campanile fragments. This possibility of sediment mixing suggests that the upper portions of the Anchor Bay member could be younger than previously thought.

The Anchor Bay sediments are distinctively greenish gray on fresh surface and contain an unusual mafic assemblage of conglomerate clasts. The sandstone is fine- to medium-grained and contains mostly plagioclase with abundant quartz and is lacking K-feldspar. The conglomerate clasts range in size from pebble to boulder and are mafic in composition with clast types including basalt, diabase, gabbro and pyroxenite. The exposed sections are 800-1700 meters thick.

The distribution of *C. orcutti* in North America is limited to west of the San Andreas fault, and the Cretaceous rocks of the Gualala Formation are the northernmost strata in which it has been found (Elder et al., 1998). Hallam (1994) determined that rudists were abundant but were rarely found north of 35°N or south of 35°S in Upper

Cretaceous strata because they were restricted to warm, reef-carbonate-producing latitudes such as where the fossils are found today.

Structure

Structural measurement and analysis is necessary in order to determine if structural features, such as folds, exist that can be used to constrain the age of remanent magnetization (i.e., using a paleomagnetic fold test). Other fabric data, such as anisotropy of magnetic susceptibility (AMS), can be corrected to a pre-folding framework for analysis with such structural data.

In the study area there is evidence that at least two tectonic events affected the Stewart's Point and Anchor Bay members of the Gualala Formation. At an indeterminate time, low-angle detachment faulting removed an unknown amount of section from the Upper Cretaceous Stewart's Point member and dropped the remaining section down onto the spilite of Black Point, the structural basement (Wentworth et al., 1998). A similar style of low-angle detachment is noted in various locations of the Great Valley Group in the Coast Ranges and constrained to the Paleocene and early Eocene (Krueger and Jones, 1989). The second event is folding of the pre-Neogene section around an east-trending axis. This was accompanied by northward verging thrust faulting. The timing is thought to be late Eocene and/or Oligocene based on lack of folding of overlying Miocene strata (Wentworth et al., 1998). A structural analysis by Tavarnelli (1998) found that the hinge of the major fold, the Black Point anticline, is horizontal. Bedding measurements from specimens that were successfully demagnetized for this study were plotted using an equal area projection (Figure 8). The fold axis determined as the pole to a best fit great circle

plunges gently west-northwest. This agrees with field measurements of fold axes in both the Stewart's Point and Anchor Bay members, but not Tavernelli's (1998) conclusion.

Sampling and Methods

Sampling

For this study, 26 sites (Figure 9) were sampled (7-24 samples per site) yielding a total of 307 cores collected from the Stewart's Point and Anchor Bay members of the Gualala Formation. Of these sites, 12 (KGS) were from the Stewart's Point member and 14 (KGA) from the Anchor Bay member. Thorough sampling of the lithologies and grain sizes of each member was made throughout the stratigraphic section on each limb of the Black Point anticline. A range of lithologies and grain sizes was selected. Samples were cored using a portable gasoline-powered drill and oriented with a magnetic compass and with a sun compass when possible. Sun compass declinations were within 3 degrees of the magnetic compass declinations. Sites were located with a global positioning system unit. Core samples were brought to the laboratory, cut into 2.2 centimeter long specimens, measured for susceptibility and its anisotropy and then stored in a magnetic-field-free room (internal field ~350nT), where paleomagnetic and rock magnetic measurements were carried out.

Paleomagnetic Measurements

After measurement of natural remanent magnetization (NRM), the specimens were subjected to detailed, step-wise, progressive demagnetization. Remanent magnetization was measured on a 3-axis 2-G 755 DC-SQUID magnetometer. Four

different methods of demagnetization were employed in an attempt to understand the remanent magnetization: 1) low temperature demagnetization (LTD), 2) alternating field (AFD) demagnetization, 3) thermal demagnetization (THD), and 4) a combination of thermal followed by AF demagnetization (THD+AFD). Low temperature demagnetization required the specimen to be immersed in liquid nitrogen in a non-magnetic dewar in the field free room. Rationale for LTD treatment will be explained below. AF demagnetization utilized a D-Tech alternating field demagnetizer and employed alternating fields of 5 to 120 mT with 5 mT steps in the 5-50 mT range, and 10 mT steps in the 50-120 mT range. Samples were demagnetized thermally in an ASC TD-48 magnetically shielded oven using steps of 5° to 50°C from room temperature to 600°C. In the combined THD+AFD method, specimens were thermally demagnetized from room temperature to 330°C followed by AFD from 5 mT to 50 mT in 5 mT steps. After each thermal demagnetization step, specimen susceptibility was measured with Bartington MS-2 susceptibility meter to check for changes in magnetic mineralogy.

Low Temperature Treatment

The low temperature demagnetization treatment performed prior to AFD, THD and THD+AFD on the majority of the specimens is intended to remove the contribution to remanence by large, multi-domain (MD) magnetite (Schmidt, 1993; Dunlop and Özdemir, 1997). Large, MD magnetite grains are commonly vulnerable to magnetic overprinting. This overprinting can mask and complicate extraction of the primary remanent magnetization. Approximately 75% of the specimens were treated with LTD. Each specimen was immersed in liquid nitrogen (T = 77 K) for 20 minutes in a non-

magnetic dewar. Specimens were then removed from the dewar and placed in the air-cooled end of the thermal demagnetizer and allowed to warm to room temperature. Each specimen's magnetization was measured and if a change in the natural remanent magnetization (NRM) of more than 10% occurred, the sample was cycled into the nitrogen again. This process was repeated until the NRM change was less than 10% for each specimen, typically about 2 to 3 treatments.

Treatment by LTD affects the physical nature of MD and MD-acting magnetite grains. LTD causes magnetite to go through a phase change at a temperature of 120 K, at which point the magnetite becomes monoclinic and the magnetocrystalline anisotropy constant becomes zero. The accompanying electrical and magnetic changes that occur at 120 K are known as the Verwey transition (Verwey, 1939). Single domain (SD) grains retain their room temperature remanence after being taken through the Verwey transition, while most of the room temperature remanence is lost in MD grains (Dunlop and Özdemir, 1997). This loss of remanence in MD grains is attributed to unpinning of domain walls from internal crystal defects during treatment (Dunlop and Özdemir, 1997). Borradaile et al. (2001) and Warnock et al. (2000) have successfully used LTD to improve the resolution of the primary remanent magnetization.

Paleomagnetic Analysis

Changes in magnetization of a rock sample during demagnetization may show up as changes in both direction and intensity. Orthogonal vector endpoint projections are used to display demagnetization data and identify components of magnetization, which show up as straight line segments along the demagnetization path. These diagrams

project the vector endpoints on a horizontal plane (Figure 10) to show declination (solid symbols) and on a vertical plane (open symbols). The latter rarely show true inclination. Data are plotted with North to the right on the positive horizontal axis and Up toward the top on the positive vertical axis.

Principal component analysis (Kirschvink, 1980) allows the directions of the straight lines to be quantified using least-squares best fits. The qualities of the line fits are estimated by the maximum angular deviation (MAD). Lines selected for analysis in this study had to have a minimum of 4 points and MAD values less than 20°.

Fisher (1953) methods were used to calculate site and member mean directions and statistics. Fisher statistics (Fisher, 1953) were developed for assessing dispersion of unit vectors on a sphere, i.e., giving unit weight to each direction. The Fisher distribution approximates a normal distribution mapped to a small area of the sphere. Paleomagnetic directional data can be plotted as unit vectors on a unit sphere using an equal area projection. Multiple factors can increase the dispersion of these data leading to scatter. A precision parameter, κ, describes the dispersion of points on a unit sphere about the true mean direction. A large κ value indicates a tight clustering of data about the mean while a κ value of 1 indicates a uniform distribution. The best estimate of κ is

$$k = (N\text{-}1)/(N\text{-}R),$$

where R is the vector sum (resultant) of the N individual unit vectors. The direction of the vector sum is the best estimate of the true mean direction. The semiangle of the cone of 95% confidence (alpha 95) can be calculated from N and R:

$$\alpha 95 = \cos^{-1}[1 - ((N\text{-}R)/R\ [(1/p)^{1/(N-1)} - 1],$$

where p is the probability level (0.05 at the commonly used 95% confidence).

Another method of evaluating the distribution of data, after Tauxe (1998), has the advantage of being applicable to non-Fisherian (e.g., "streaked" and/or non-normal) data distributions. This method involves first calculating an orientation matrix for the data to get associated eigenvectors and eigenvalues. Then the geographic coordinates are transformed into a 'data' coordinate system that centers the data about the principal eigenvector, as opposed to centering about a vertical axis. The relevant clustering parameter in these statistics is the value of the maximum eigenvalue of the orientation matrix. The greater this value, the greater the directional clustering.

A method of determining confidence regions around a mean direction that does not require a particular distribution is the statistical bootstrap method. Multiple, synthetic para-data sets are generated that reflect the variability of the observed data set. The major assumption with the bootstrap method is that the original data set represents the full distribution possibilities. A confidence region, e.g., at 95%, can be defined as the ellipse that encompasses 95% of the directions calculated from these para-data sets.

The mean pole for the Late Cretaceous was determined by combining the poles of the Gunderson and Sheriff (1991) and Diehl (1991) studies for Late Cretaceous volcanics. GMAP was then used to calculate the expected Late Cretaceous direction (Table 1) for the Gualala Formation at its present location relative to cratonic North America.

Field Tests

A fold test is used to determine the age of the magnetization relative to the age of folding. If a rock has retained a primary magnetization through a folding event, the magnetic directions will cluster better after correction to paleohorizontal. Since

paleomagnetic vectors are rarely perfectly parallel, a statistical test is necessary to determine when clustering is best. Tauxe and Watson's (1994) bootstrap fold test is less dependent on an assumed distribution than is the classic McFadden (1990) fold test. The Tauxe and Watson (1994) bootstrap fold test involves the creation of an orientation matrix and the tightness of grouping is reflected in the relative magnitudes or the eigenvalues (τ). The behavior of $\tau 1$ (the largest eigenvalues from the orientation matrix) during unfolding reveals the correction where the grouping is tightest. A 95% confidence interval is then determined by the bounds of 95% of the distribution of the generated para-data set results.

Fabric Measurement Methods

Anisotropy of magnetic susceptibility (AMS) was measured for all samples, before the paleomagnetic measurements, using a KLY-3 Kappabridge Spinning Magnetic Susceptibility Anisotropy meter. AMS quantifies the minerals' preferred orientation in a specimen and thus can provide a quantified measure of mineralogic fabric. Applications of these data include, but are not limited to, the determination of paleocurrent directions and strain analysis. The data were reduced with the program SUSAR provided with the instrument and then plotted with their site means and bootstrap confidence ellipsoids using Tauxe's (1998) *plotams* and *bootams* paleomagnetic software programs. Flinn (1962) plots were created to graphically portray tensor shape.

Magnetic Properties Methods

Characterization of the magnetic mineralogy of the samples from the Anchor Bay and Stewart's Point member was achieved using multi-component isothermal remanent magnetization (Lowrie, 1990) and hysteresis parameters. The Lowrie method distinguishes between the magnetic carriers magnetite, pyrrhotite and hematite. Hysteresis parameters are controlled by mineralogy and grain size and indicate whether the specimen contained superparamagnetic, single-domain, pseudo-single-domain or multidomain magnetite.

The Lowrie (1990) method requires imparting a multi-component isothermal remanent magnetization (mIRM) to the specimen in three orthogonal directions such that each axis of a specimen is magnetized in a different part of the specimen's coercivity spectrum. This is followed by thermal demagnetization. The unblocking temperatures of the different mIRM components of each sample indicate the magnetic mineralogy (Lowrie, 1990). For this study an ASC pulse magnetizer was employed to provide a 2.5 T field along the specimen Z-axis, a 0.2 T field along the Y-axis and 0.02 T field along the X-axis. Hematite has coercivity greater than 1 T and an unblocking temperature of ~670°C. Single-domain pyrrhotite has a coercivity between 0.4 T and 1 T and an unblocking temperature of ~320°C. Larger pyrrhotite and magnetite have coercivities below 0.3 T and unblocking occurs at 320°C (pyrrhotite) or up to 580°C (magnetite).

Hysteresis loops are generated by subjecting a small sample to a magnetic field that is cycled from a large value in one direction ($+H_{max}$), to the same strength in the opposite direction ($-H_{max}$) and back. The magnetization of the magnetic minerals in the

sample is observed during the cycling. Parameters used to describe the hysteresis loops include the remanence when the applied field is zero (M_r saturation remanent magnetization), the maximum magnetization achieved when the applied field exceeds the coercivities of all magnetic grains (M_s saturation magnetization), the coercivity of the magnetic grains when the applied field is zero (H_c bulk coercivity), and the strength of the reverse field necessary to achieve zero magnetization after saturation (H_{cr} coercivity of remanence) (Figure 11).

Magnetic hysteresis curves were obtained for 4 samples at the University of Minnesota's Institute for Rock Magnetism, using a Princeton Measurements model 3900-4 VSM with applied fields of up to 1.5 T.

Results

Paleomagnetic Results

Demagnetization for both the Stewart's Point member and Anchor Bay member was completed with the methods explained above. No single method proved ideal so the final analysis includes data from all methods.

Low temperature demagnetization reduced magnetic intensity 0% to 79%. All specimens were retained for further treatment after LTD.

Ninety two out of 309 specimens were demagnetized with AFD. Of these, 76 specimens were discarded after changes in magnetization became too erratic to define linear segments on orthogonal vector plots after low level (0-20mT) AFD (Figure 10a). For the remaining 26 specimens that had smooth demagnetization paths, the junction point between first and second removed components occurred at about 25mT and second

removed components were defined from 25 mT to 100mT.

Most (102 out of 106) of the specimens treated with THD, regardless of whether LTD treatment proceeded it, exhibited increased intensity and susceptibility between 320°C and 450°C. At this point, the demagnetization paths became extremely erratic (Figure 12a) and the specimens were removed from consideration. Reasons for increased susceptibility and erratic demagnetization paths include thermal alteration of sulfide minerals to magnetite during the thermal demagnetization process. For specimens with smooth demagnetization paths, first components were fit up to 200°C and second components from 530°C to 580°C.

The last demagnetization method employed utilized LTD followed by THD only to 320°C, in an attempt to avoid the magnetic mineralogy changes occurring during THD at temperatures above 320°C, and then AFD. Twenty of 111 specimens treated this way displayed suitably smooth demagnetization paths allowing extraction of a second-removed component during AFD for some specimens (Figure 13b). First removed components were recovered up to 200°C while second removed components were over the 20-60mT range of AFD.

Well-defined results were not plentiful enough from each site to calculate mean directions on a site by site basis, so all specimens with a well-defined second removed component were analyzed together in either Stewart's Point or Anchor Bay groups. Potential problems arise with the comparison of AFD data with THD only and THD and AFD combination data. AFD might be isolating pyrrhotite at high fields, whereas the THD and THD+AFD methods, at high temperatures, may be selecting for magnetite. The remanence carried by the pyrrhotite was likely acquired during alteration and the

magnetite potentially carries the detrital remanence. The mixing of all demagnetization data when calculating mean directions was validated by analyzing AFD only data with the Tauxe and Watson (1994) fold test (Figure 14) and noting no difference when compared to fold test data from THD and THD+AFD methods (Figures 15, 16, 17 and 18).

Stewart's Point member mean directions

Of the 157 demagnetized specimens from the Stewart's Point member, 30 have well defined second-removed components of magnetization. The first removed components of magnetization (Figure 15; Table 1) of these specimens fail the Tauxe and Watson (1994) fold test with minimum dispersion of directions at approximately -7% and maximum at 100%, where 100% unfolding is fully tilt corrected. The second removed components, when corrected for folding (Figure 16; Table 1), fail the Tauxe and Watson (1994) fold test at 95% confidence. The maximum clustering of the directions occurring at 0% unfolding with a confidence interval from -13% to 22% unfolding.

Anchor Bay member mean directions

Of 152 specimens from the Anchor Bay member demagnetized, 20 specimens yielded a well-defined second-removed component. The first removed components from these specimens (Figure 17; Table 1) fail the Tauxe and Watson (1994) fold test with maximum clustering of the directions at -20% unfolding, with 95% confidence intervals between -32% and 0% unfolding.

The second removed component is of normal polarity with moderate to steep inclinations and northward declinations. The second removed components (Figure 18; Table 1) also fail the Tauxe and Watson (1994) fold test with maximum clustering of the directional data occurring at -25%, with the 95% confidence intervals between -38% and -2% unfolding.

Magnetic Fabric Results

Flinn (1962) plots of AMS data indicate that nearly all sites contain oblate fabrics (Figure 19). Equal area plots of AMS data after correcting for bedding indicate that the minimum susceptibility axes (k-min) cluster within 10° of the vertical axis, and maximum susceptibility axes (k-max) lie near the horizontal plane (Figure 20). The k-max axes are scattered and not consistent with being a fold axis lineation indicating no significant mineral reorientation or growth during deformation so the fabric is presumed to be depositional.

Magnetic Properties Results

Representative results for the Lowrie (1990) tests are shown in Figure 21a and 21b. Most of the remanence was along the y-axis, which was magnetized from 0.200T to 0.020T. This magnetization experienced a large drop during thermal demagnetization from 570°C to 590°C. The combination of the coercivity range and unblocking temperature range indicates that magnetite carried this remanence. A drop in magnetization also occurred in specimen KGS0311A at approximately 330°C. This

drop, along with an increase in susceptibility at 330°C in 96% of the specimens treated with THD, is consistent with the presence of pyrrhotite.

The parameters determined from the hysteresis curves (Figure 22) for the Stewart's Point and Anchor Bay members are shown on the modified Day plot of Dunlop (2002) in Figure 23. Three of the four specimens' data plot along the boundary of pseudo-single-domain magnetite (PSD) and a single domain (SD) and multidomain (MD) mixture, while the fourth specimen is clearly superparamagnetic and was not included. A comparison with experimental data for sized PSD and theoretical SD + MD mixing curves (Figure 24) indicate magnetite grain size possibly ranges from 0.39μm to 0.76μm. Unfortunately, material for hysteresis experiments had to be selected before results of remanence studies were available, and all are from samples that yielded no useful results. Therefore, these hysteresis data may not reflect magnetic mineralogy of samples with useful remanence.

Discussion

Samples from each member of the Gualala Formation have first-removed components that fail the fold test and whose in situ directions are not far from the expected present day direction of the earth's magnetic field (Figure 25; table 1).

Both members have second-removed paleomagnetic directions that fail the fold test at 95% confidence, with the maximum clustering of directions occurring between 0% and -38% unfolding. The *in situ* second removed components are approximately 15-25 degrees clockwise of the direction expected for in situ magnetization in the Late Cretaceous (Figure 26). The negative unfolding results may be attributed to the

plunge of the fold or possible differential rotation after remagnetization.

These results clearly indicate that the Gualala Formation has been remagnetized following folding. All of the rocks in this study have normal polarity, which suggests that the remagnetization took place either over a short period of time (within one normal-polarity chron, the longest of which is ca 2 Ma for post-75 Ma time) or during the Cretaceous Normal Superchron. If the latter is true the paleontologically constrained Paleocene age for the Anchor Bay member, while not ruled out by exclusively normal polarity results, is suspect. The fact that the Gualala Formation rocks are not metamorphosed does rule out significant reheating as a cause of remagnetization. However, some insights into this process may be gained by examining occurrences of remagnetization in other units from this region.

In all the cases reviewed in the introduction (Mankinen, 1987; Frei and Blake, 1998; Hagstrum and Jones, 1998) and in this study, remagnetization via orogenic fluid circulation or crystallization remanent magnetization (CRM), in these rocks is suspected. The AMS data indicates that k-max does not appear to be from an intersection lineation and therefore remagnetization is not related to physical deformation during folding. Both pyrrhotite and magnetite carry the remagnetization, which suggests that reduction of magnetite related to fluid chemistry occurred. It is becoming clear that similar types of remagnetizations can occur in clastic rocks during deformation of convergent/strike slip margins.

Paleomagnetic results for the Point Arena terrane are similar to the remagnetization results from the Late Cretaceous sedimentary rocks of Mt. Diablo (Hagstrum and Jones, 1998; Figure 27 and Figure 28). A Late Cretaceous

remagnetization is postulated in these studies because only normal magnetizations were found. A discussion with Dave Engebretson revealed that the slab window between the Kula and Farallon plates (see Figure 27) was under the North American margin at the same time as the initiation of the San Andreas fault and the extrusion of the Iverson Basalt (Figure 4) onto the Point Arena terrane. The *in situ* second removed components from the overlying Oligocene Iverson basalt, when changed from reverse to normal polarity, match the Stewart's Point and Anchor Bay members second removed directions (Figure 29) and indicate an Oligocene remagnetization.

Conclusions

Many of the sedimentary units that were accreted during the Upper Cretaceous in the area that is now Northern California appear to be affected by alteration after deposition. The mechanism may be the percolation of orogenic fluids during, or directly after, folding that were caused by basalt flows from material generated by the slab window as it was being subducted under North America. This regional signature may yield future insights into the timing of deformation.

Resolution of the origin of the remagnetization of these clastic rocks will require further rock-magnetic tests and petrographic analysis to completely characterize their magnetic mineralogy. A combination of hysteresis measurements and Curie temperature determinations would be useful to characterize the carriers of remagnetization. Petrographic analyses would determine the amount of alteration of silicate minerals, the presence of solution and/or precipitation along grain boundaries, and the presence

of mineral overgrowths. Other pursuits could include the determination of clay maturation and organic content maturation.

References

Addis, K., 2004, Paleomagnetism of the Eocene German Rancho formation, Point Arena Terrane, California: Masters thesis, Western Washington University.

Beck, M. E., and Noson, L., 1972, Anomalous paleolatitudes in Cretaceous rocks, *Nature: Ph ysical Science (London), 235*, 11-13.

Bogue, S. W., Cowan, D. S., and Garver, J. I., 1989, Paleomagnetic evidence for poleward transport of Upper Jurassic rocks in the Decatur terrane, San Juan Islands, Washington, *Jour. Geophys. Res., 94,* 10415-10427.

Borradaile, G. J., Lagroix, F. and Trimble, D., 2001, Improved isolation of archeomagnetic signals by combined low temperature and alternating field demagnetization: *Geophys. J. Int., 147*, 176-182.

Brandon M. T., Cowan, D. S., and Vance, J. A., 1988, The Late Cretaceous San Juan thrust system, San Juan Islands, Washington: Geol. *Soc. Am. Spec. Pap. 221*, 81.

Burmester, R. F., Blake, Jr., M. C., and Engebretson, D. C., 2000, Remagnetization during Cretaceous Normal Superchron in Eastern San Juan Islands, WA: implications for tectonic history: *Tectonophysics, 326*, 73-92.

Butler, R. F., Gehrels, G., and Kodama, K. P., 2001a, A moderate translation alternative to the Baja British Columbia hypothesis: *GSA Today, 11*(6), 4-10.

Champion, D. E., Howell, D. G., and Grommé, S., 1984, Paleomagnetic and geologic data indicating 2500 km of northward displacement for the Salinian and related terranes, California: *J. Geophy. Res., 89*, 7736-7752.

Coney, P. J., Jones, D. L. and Monger, J. W. H., 1980, Cordilleran suspect terranes: *Nature (London), 288*, 329-333.

Cowan, D. S., Brandon, M. T., and Garver, I. J., 1997, Geologic tests of hypotheses for large coastwise displacements-A critique illustrated by the Baja British Columbia controversy: *Am. J. Sci., 297*, 117-173.

Dickinson, W. R. and Butler, R. F., 1998, Coastal and Baja California paleomagnetism reconsidered: *Geol. Soc. Am. Bull., 110*, 1268-1280.

Diehl, J. F., 1991, The Elkhorn mountains revisited; new data for the Late Cretaceous paleomagnetic field of North America: *Jour. Geophy. Res., 96*, 9887-9894.

Dunlop, D. J., 2002, Theory and application of the Day plot (M_{rs}/M_s versus H_{cr}/H_c) 1. Theoretical curves and tests using titanomagnetite data: *Jour. Geophys. Res., 107*, B3, 22 p.

Dunlop, D. J. and Özdemir, Ö., 1997, Rock magnetism: fundamentals and frontiers: Cambridge, Cambridge University Press, 573 p.

Durham, J. W. and Kirk, M. V., 1950, Age of the Coralliochama beds of the Pacific Coast: *Geo. Soc. of Am. Bul., 61*, p. 1537.

Elder, W. P., Saul, L. R. and Powell, II, C. L., 1998, Late Cretaceous and Paleogene molluscan fossils of the Gualala block and their paleogeographic implications: Pacific Section SEPM, 84, 149-159.

Enkin, R. J., Baker, J. and Mustard, P. S., 2001, Paleomagnetism of the Upper Cretaceous Nanaimo Group, southwestern Canadian Cordillera: *Can. Jour. Earth Sci., 38*, 1403-1422.

Fisher, R., 1953, Dispersion on a sphere: Proceedings of the Royal Society of London, A., 217, 295-305.
Flinn, D., 1962, On folding during three-dimensional progressive deformation: *Geol. Soc. Of London Quar. Jour., 118*, 385-433.
Frei, L. S. and Blake, Jr., M. C., 1987, Remagnetization of the Coast Range ophiolite and lower part of the Great Valley sequence in Northern California and Southern Oregon: *Jour. Geoph. Res., 92*, 3487-3499.
Gunderson, J. A. and Sheriff, S. D., 1991, A new Late Cretaceous paleomagnetic pole from the Adele mountains, west central Montana: *Jour. Geophy. Res., 96*, 317-326.
Hagstrum, J. T. and Jones, D. L., 1998, Paleomagnetism, paleogeographic origins, and uplift history of the Coast Range ophiolite at Mount Diablo, California: *Jour. Geoph. Res., 103*, 383-390.
Hallam, A., 1994, An outline of Phanerozoic biogeography: Oxford, UK, Oxford University Press, 246 p.
Housen, B. A., Beck Jr., M. E., and Burmester, R. F., 2003, Paleomagnetism of the Mount Stuart Batholith revisited again; what has been learned since 1972?: *Am. J. Sci., 303*(4), 263-299.
Hults, C. K. and Housen, B. A., 2000, Paleomagnetism of the Jura-Cretaceous Kyuquot Group, Vancouver Island, British Columbia: Masters thesis, Western Washington University.
Irving, E., 1985, Tectonics; whence British Columbia?: Nature (London), 314, 673-674.
Kanter, L. R., 1983, Paleomagnetic constraints on the movement history of Salinia: Doctoral Dissertation, Stanford University.
Kanter, L. R., and Debiche, M., 1985, Modeling the motion histories of the Point Arena and central Salinia terranes, in Howell, D. G., ed., Tectonostratigraphic terranes of the Circum-Pacific region: Houston, Texas, *Circum-Pacific Council for Energy and Mineral Resources Earth Science Series, 1*, 85-108.
Kirschvink, J. L., 1980, The least-squares line and plane and the analysis of paleomagnetic data: *Geophys. Jour. Of the Royal Acad., 62*, 699-718.
Kodama, K. P. and Ward, P. D., 2001, Compaction-corrected paleomagnetic paleolatitudes for Late Cretaceous rudists along the Cretaceous California margin: Evidence for less than 1500 km of post-Late Cretaceous offset for Baja British Columbia: *Geol. Soc. of Am., 113*, 1171-1178.
Krueger, S. W. and Jones, D. L., 1989, Extensional fault uplift of regional Franciscan blueschists due to subduction shallowing during the Laramide Orogeny: *Geology, 17*, 1157-1159.
Lowrie, W., 1990, Identification of ferromagnetic minerals in a rock by coercivity and unblocking temperature properties: *Geophys. Res. Let., 17*, 159-162.
Mankinen, E. A. and Irwin, W. P., 1982, Paleomagnetic study of some Cretaceous and Tertiary sedimentary rocks of the Klamath Mountains province California, *Geology, 10*, 82-87.
McCabe, C. and Channel, J. E. T., 1994, Late Paleozoic remagnetization in limestones of the Craven Basin (northern England) and the rock magnetic fingerprint of remagnetized sedimentary carbonates: *Jour. Geophy. Res., 99*, 4603-4612.
McDougall, K., 1998, Paleogene foraminifera of the Gualala block and their relation to

local and global events: Pacific Section, SEPM, 84, 3-26.
Monger, J. W. H. and Price, R. A., 1996, Comment on "Paleomagnetism of the Upper Cretaceous strata of Mount Tatlow: Evidence for 3000 km of northward displacement of the eastern Coast Belt, British Columbia" by P. J. Wynne et al., and on "Paleomagnetism of the Spences Bridge Group and northward displacement of the Intermontane Belt, British Columbia: A second look" by Irving et al.: *J. Geophs. Res., 101*, 13,793-13,799.
Muttoni, G., Kent, D. V., and Orchard, M., 2001, Paleomagnetic reconnaissance of early Mesozoic carbonates from Williston Lake, northeastern British Columbia, Canada: evidence for late Mesozoic remagnetization: *Can. Jour. of Earth Sci., 38*, 1157-1168.
Schmidt, P. W., 1993, Palaeomagnetic cleaning strategies: *Phys. of the Earth and Plan. Int., 76*, 169-178.
Schott, R. C., Johnson, C. M., and O'Neil, J. R., 2004, Late Cretaceous tectonic history of the Sierra-Salinia-Mojave arc as recorded in conglomerates of the Upper Cretaceous and Paleocene Gualala Formation, northern California: *J. Geophys. Res., 109*, B02204.
Tauxe, L., 1998, Paleomagnetic principles and practice, modern approaches in geophysics: Kluwer Academic Publishers, v. 17, 299 p.
Tauxe, L. and Watson, G., 1994, The fold test: an eigen analysis approach, *Earth Planet. Sci. Lett.*, 122, 331-341.
Tavarnelli, E., 1998, Tectonic evolution of the northern Salinian Block, California, USA; Paleogene to Recent shortening in a transform fault-bounded continental fragment: *Geol. Soc. Spec. Pubs., 135*, 107-118.
Verwey, E. J., 1939, Electronic conduction of magnetite (Fe_3O_4) and its transition point at low temperature: *Nature, 144*, 327-328.
Ward, P. D., Hurtado, J. M., Kirschvink, J. L., and Verosub, K. L., 1997, Measurements of the Cretaceous paleolatitude of Vancouver Island; Consistent with the Baja-British Columbia hypothesis: *Science, 277*, 1642-1645.
Warnock, A. C., Kodama, K. P. and Zeitler, P. K., 2000, Using thermochronometry and low-temperature demagnetization to accurately date Precambrian paleomagnetic poles: *J. Geophys. Res., 105*, 19,435-19,453.
Weaver, C., 1944, Geology of the Cretaceous (Gualala Group) and Tertiary formations along the Pacific coast between Point Arena and Fort Ross, California: University of Washington Publications in Geology, 6, no. 1, 29 p.
Wentworth, C. M., 1966, The Upper Cretaceous and Lower Tertiary rocks of the Gualala area, northern Coast Ranges, California: Ph.D. thesis, Stanford University Publications, Geological Sciences, v. 11, 130-143.
Wentworth, C. M., Jones, D. L., and Brabb, E. E., 1998, Geology and regional correlation of the Cretaceous and Paleogene rocks of the Gualala Block, California: Pacific Section, SEPM, 84, 3-26.
White, C. A., 1885, On new Cretaceous fossils from California: U.S. Geological Survey Bulletin 22.
Wynne, P. J., Irving, E., Maxson, J. A., and Kleinspehn, K. L., 1995, Paleomagnetism of the Upper Cretaceous strata of Mount Tatlow; evidence for 3000 km of northward displacement of the eastern Coast Belt, British Columbia: *Jour. Geoph. Res., B, Solid Earth and Plan., 100*, 6073-6091.

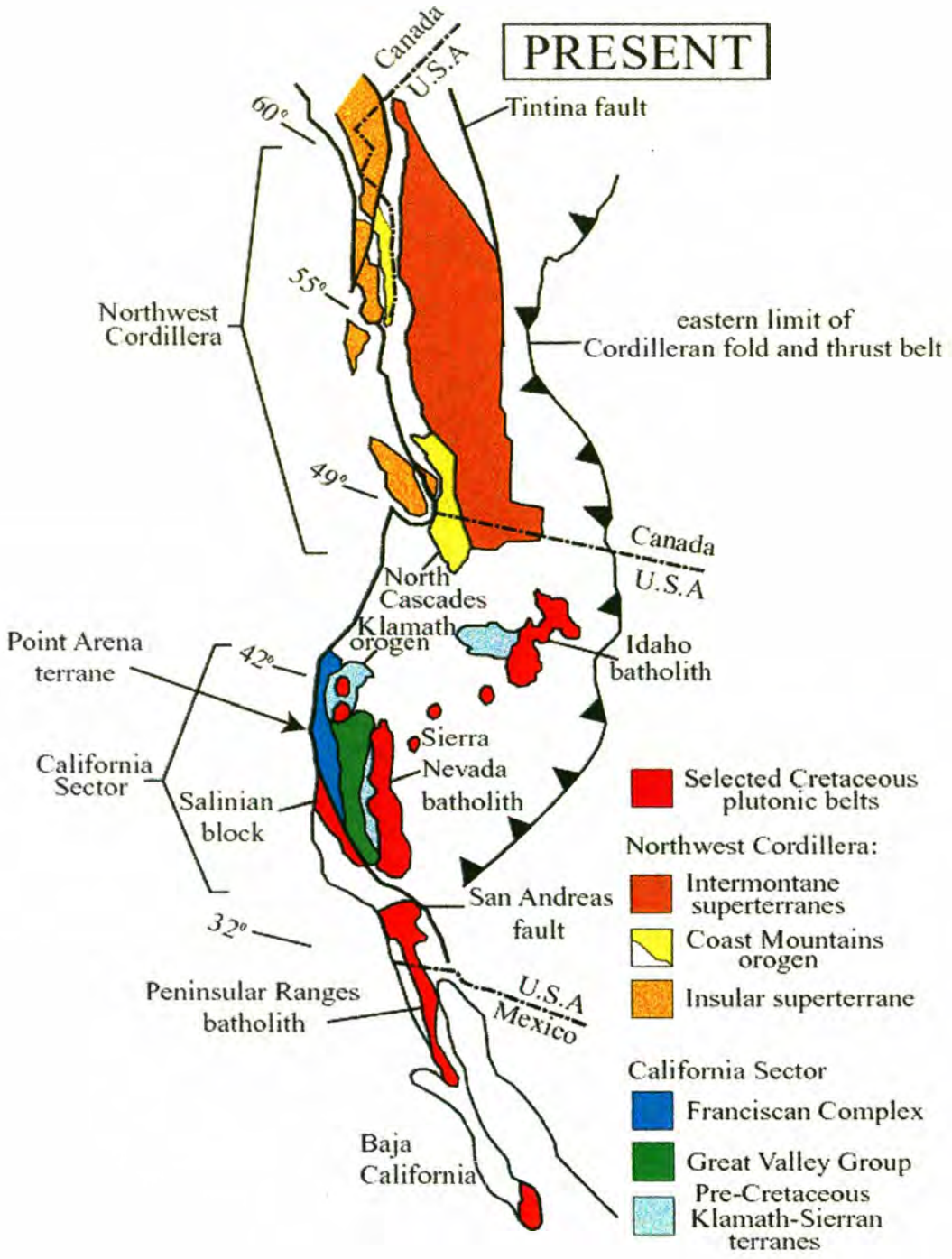

Figure 1. Present day terrane map of western North America (modified from Cowan et al., 1997).

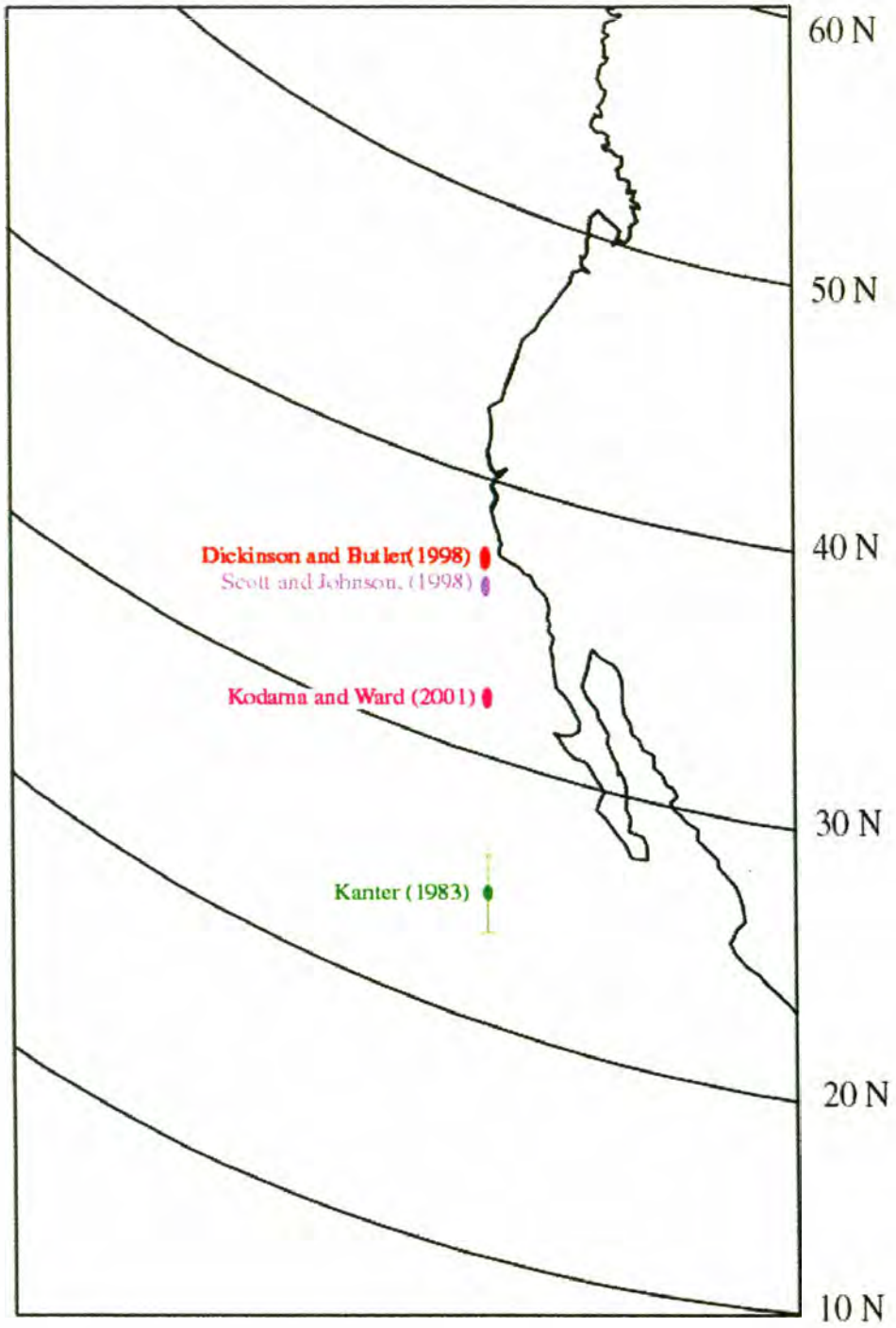

Figure 2. Cretaceous paleolatitudes estimated for the Point Arena terrane by different authors. North American craton at restored latitude using the Diehl (1991) and Gunderson and Sheriff (1991) combined reference poles (modified from Addis, 2004).

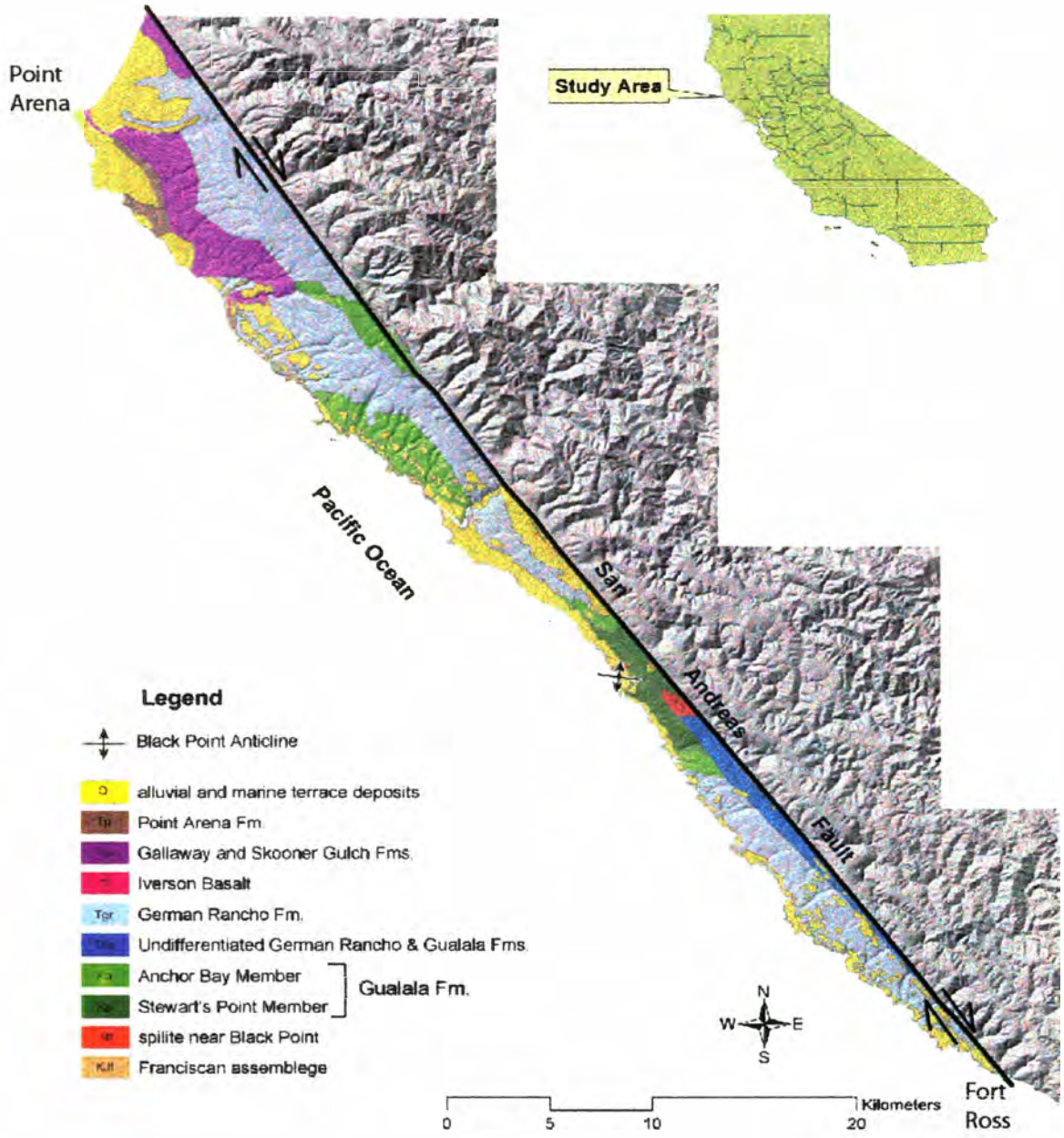

Figure 3. Geologic map of Point Arena terrane (Compiled by Katherine Kelleher from Wentworth, 1966; USGS 1986; Wentworth, 1998. DEMs from USGS, 1998).

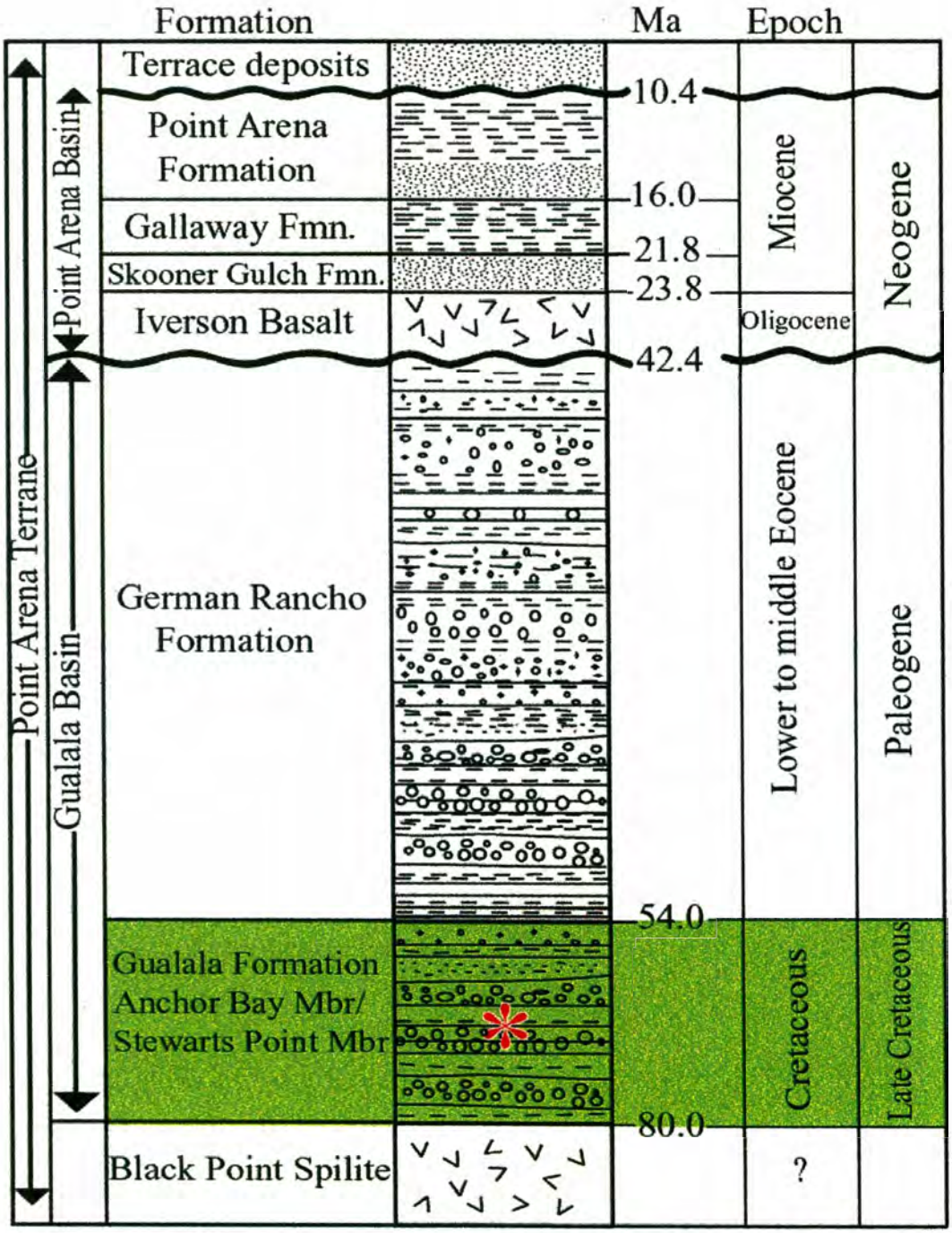

Figure 4. Stratigraphic section of the Point Arena terrane. Red asterisk denotes location of the rudist *Coralliochama Orcutti* (modified from Addis, 2004 and Wentworth, 1966).

Figure 5. Coastal exposures of Anchor Bay member north of Fort Ross (top, facing south) and Stewart's Point member (bottom, facing north) at Stengel Beach. Stewart's Point exposure is approximately 15m high.

Figure 6. View facing northeast at spilite exposure at Black Point, CA. Cliff height is 20m.

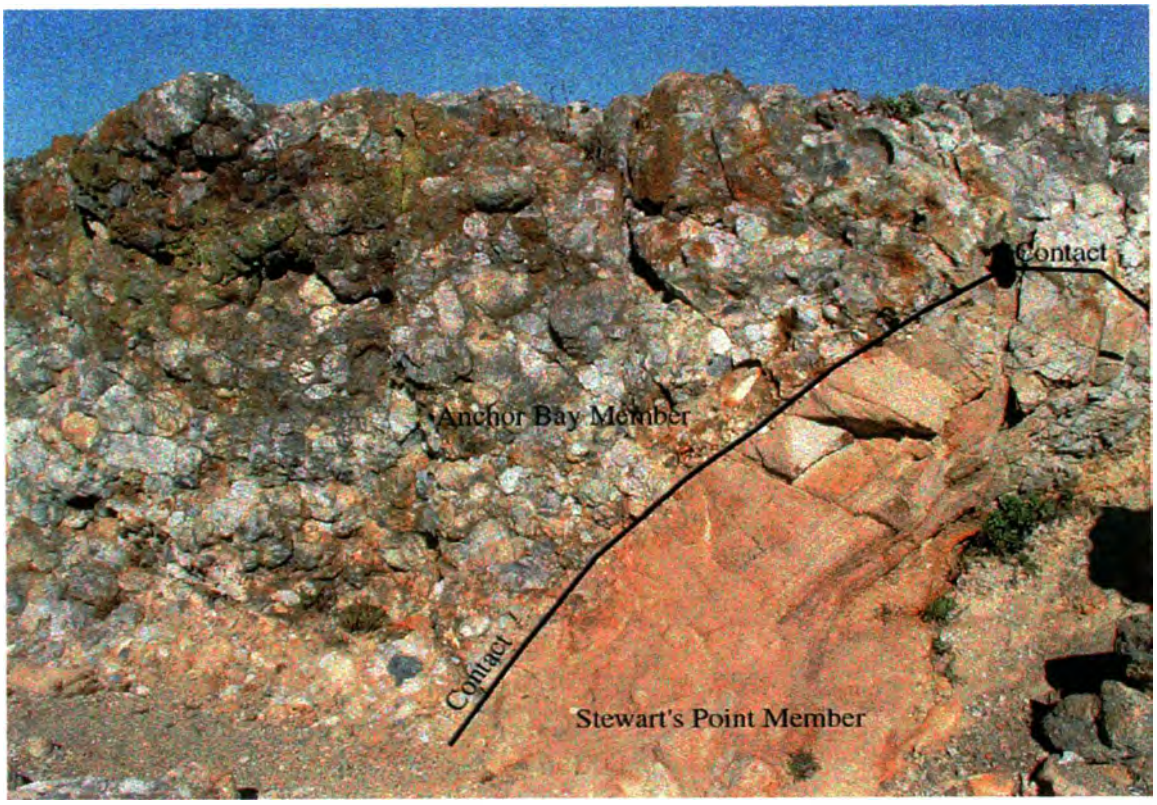

Figure 7. View facing northeast at the conformable contact of Stewart's Point and Anchor Bay members at Stewart's Point, CA. Cliff face is 15m tall.

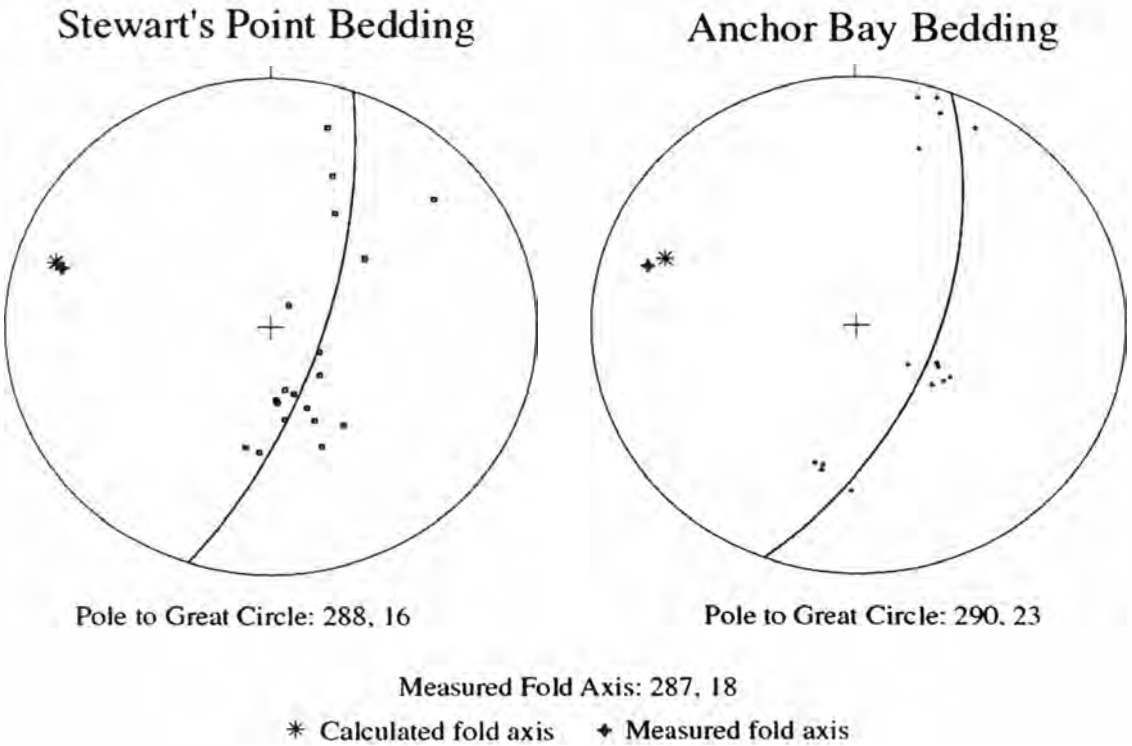

Figure 8. Equal area plots of poles to bedding for successfully demagnetized specimens. Poles to great circle fit to the bed poles (plotted as asterisk), are close to measured fold axes (plotted as +).

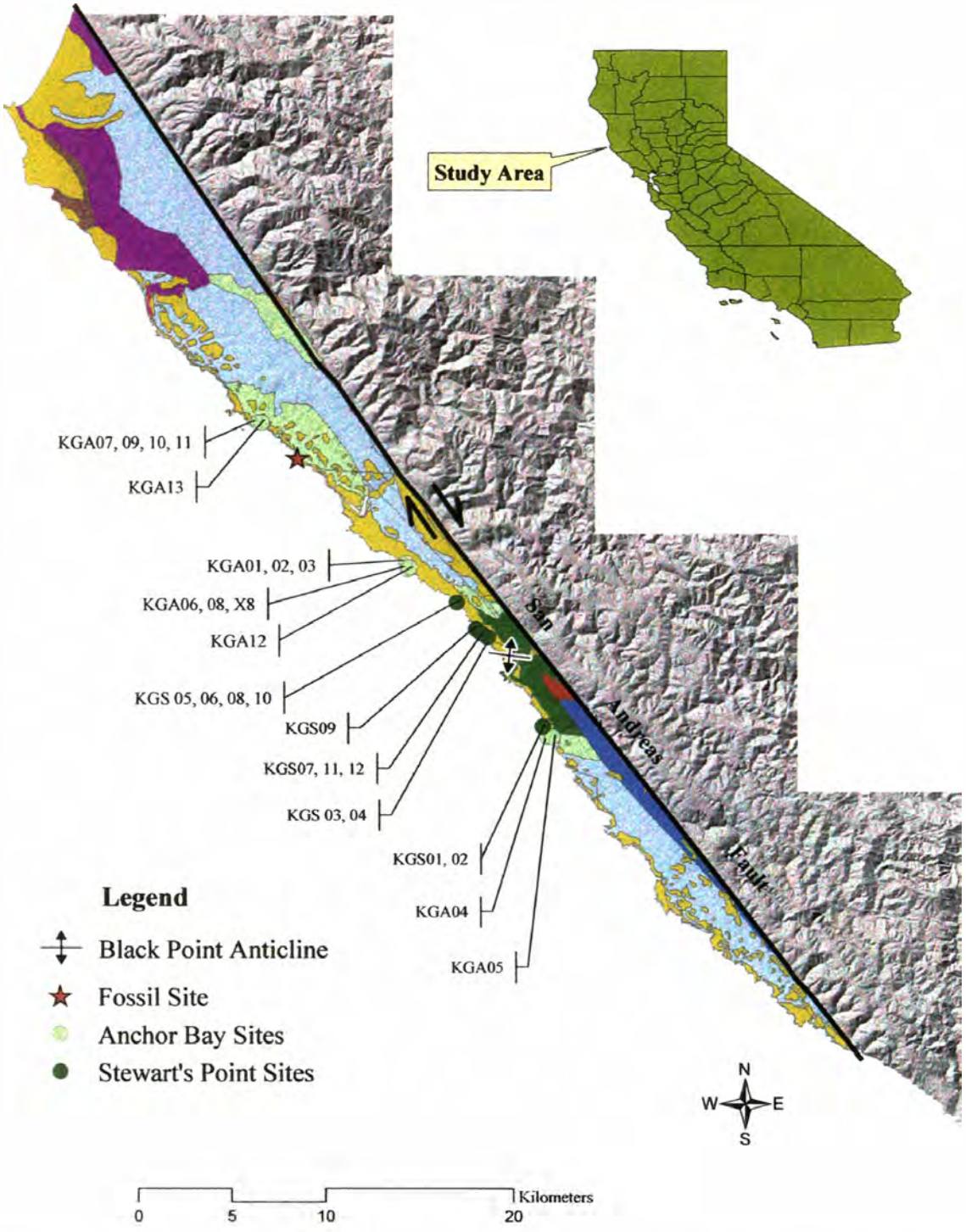

Figure 9. Map indicating sampling locations within the Stewart's Point and Anchor Bay members of the Gualala Formation. Base map compiled by Katherine Kelleher from Wentworth (1966), USGS (1986), Wentworth (1998). DEMs from USGS (1998). Color code same as Figure 3.

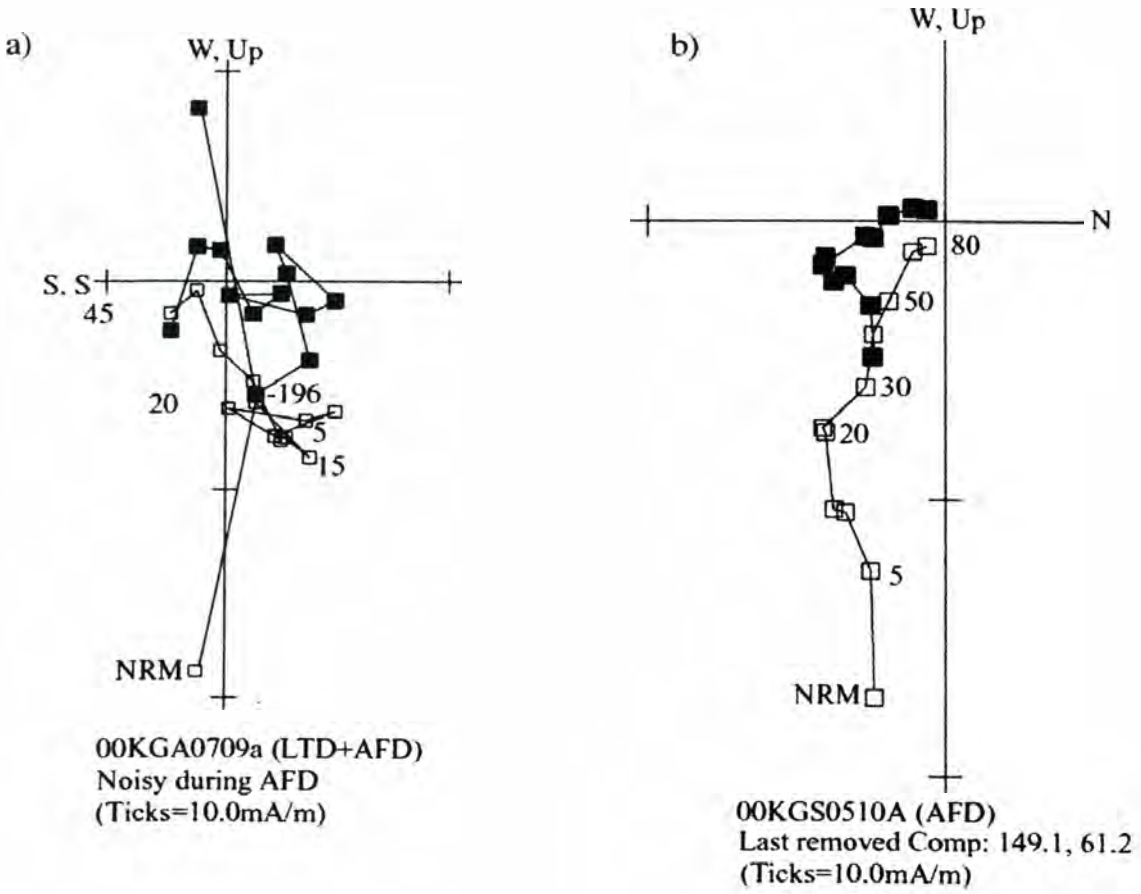

Figure 10. Orthogonal plots of AFD, steps listed in miliTesla. Open (filled) symbols denote vertical (horizontal) projection of vectors. All plots in geographic coordinates. a) has first step at -196, indicating LTD treatment, and shows an unsuccessful recovery of a second component. b) shows successful two component AFD.

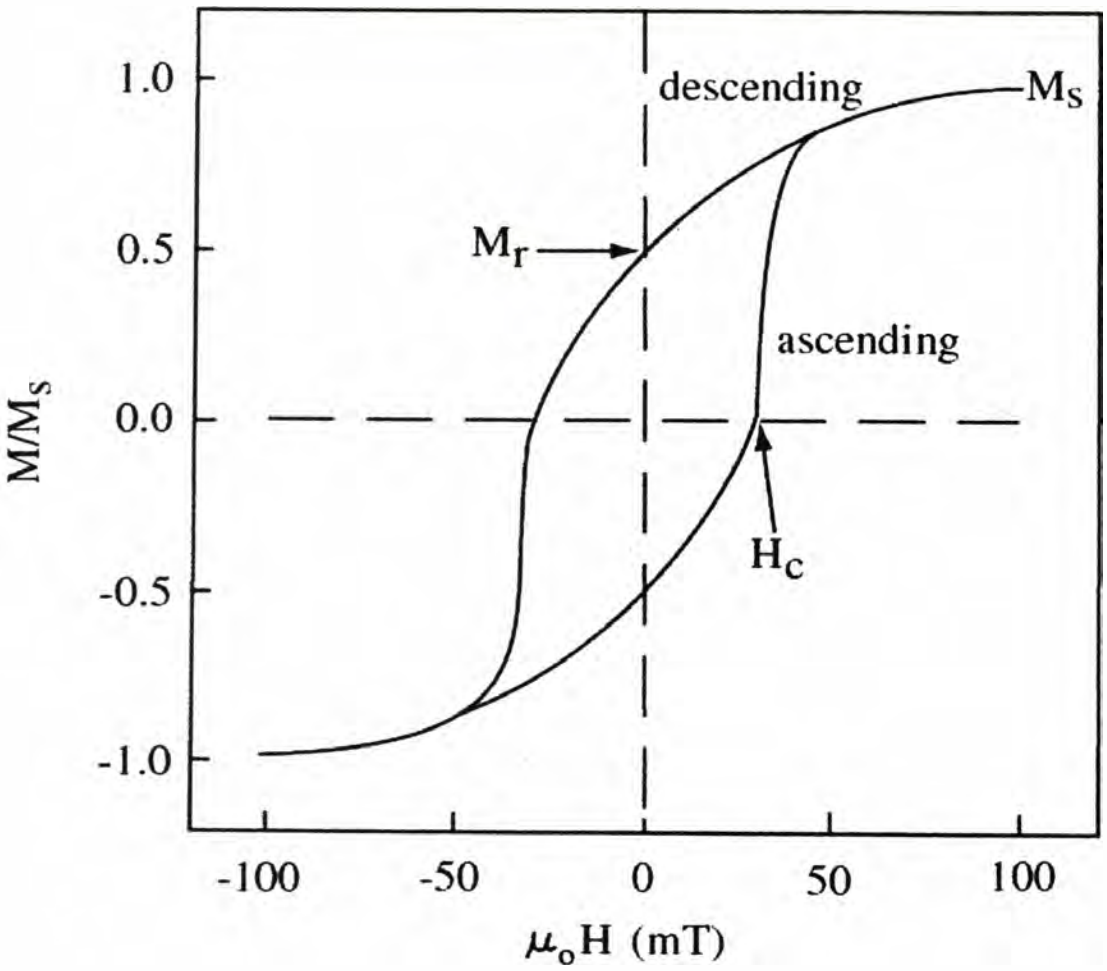

Figure 11. Sample hysteresis loop indicating Mr (saturation remanent magnetization), Ms (saturation magnetization), and Hc (bulk coercivity), after Tauxe (1998).

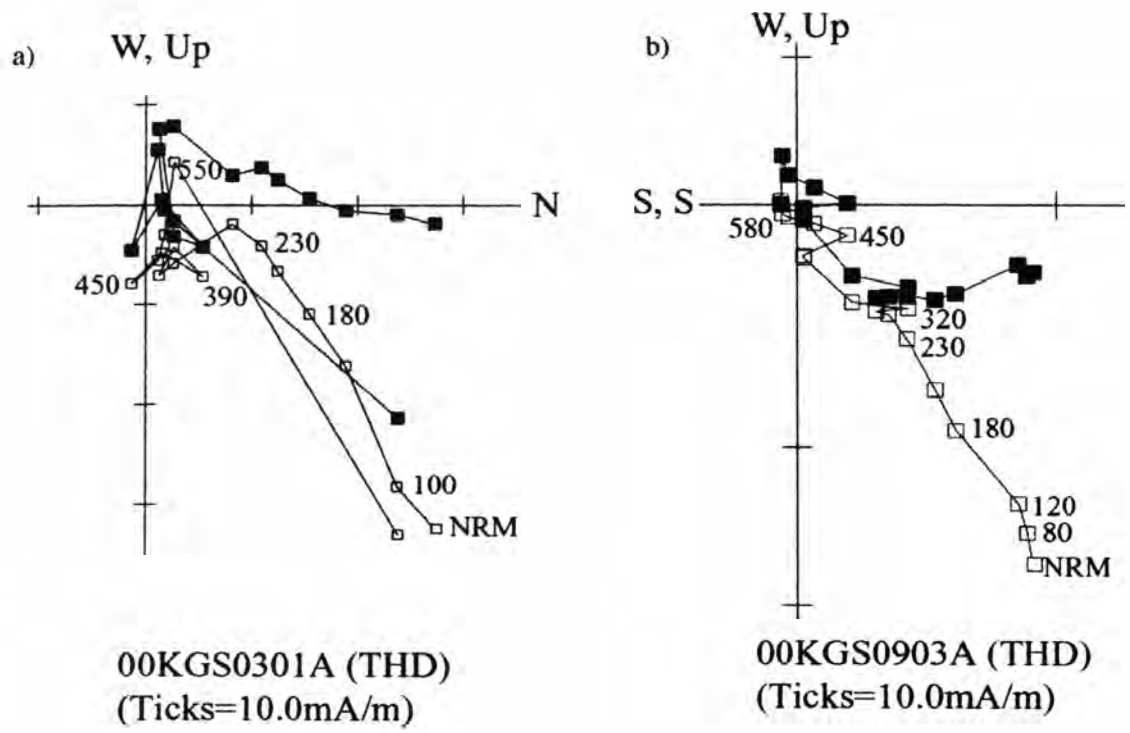

Figure 12. Orthogonal plots of THD with steps in degrees C. Open (filled) symbols denote vertical (horizontal) projections of the vectors. Both plots in geographic coordinates. Unsuccessful (a) and successful (b) examples of demagnetization.

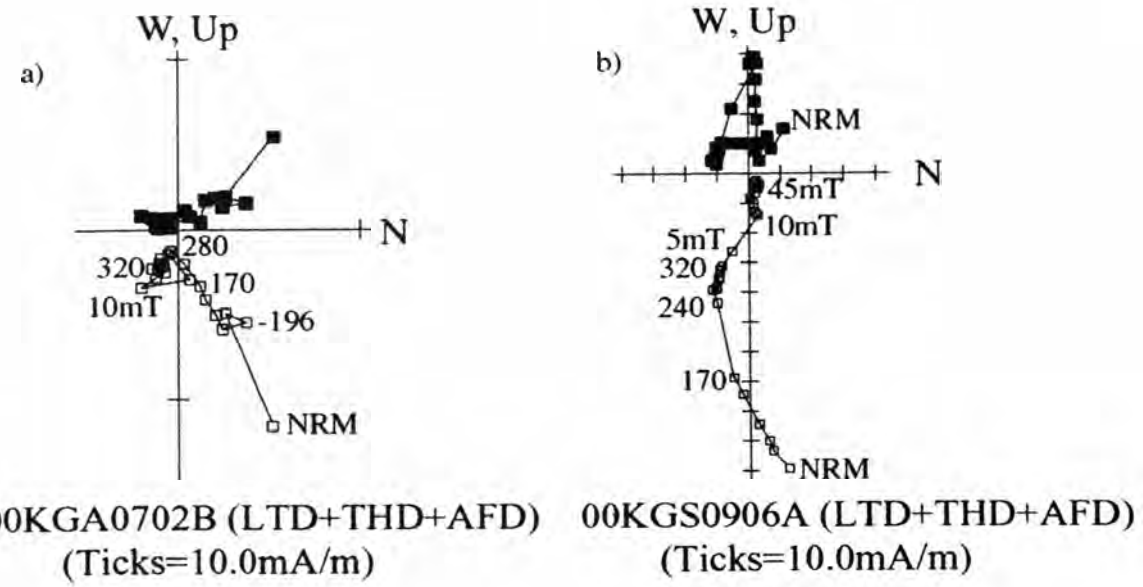

Figure 13. Orthogonal plots of the combination method. Unlabeled numbers indicate steps in degrees C. Open (filled) symbols denote vertical (horizontal) projections of the vectors. Both plots in geographic coordinates. Unsuccessful (a) and successful (b) examples of demagnetization.

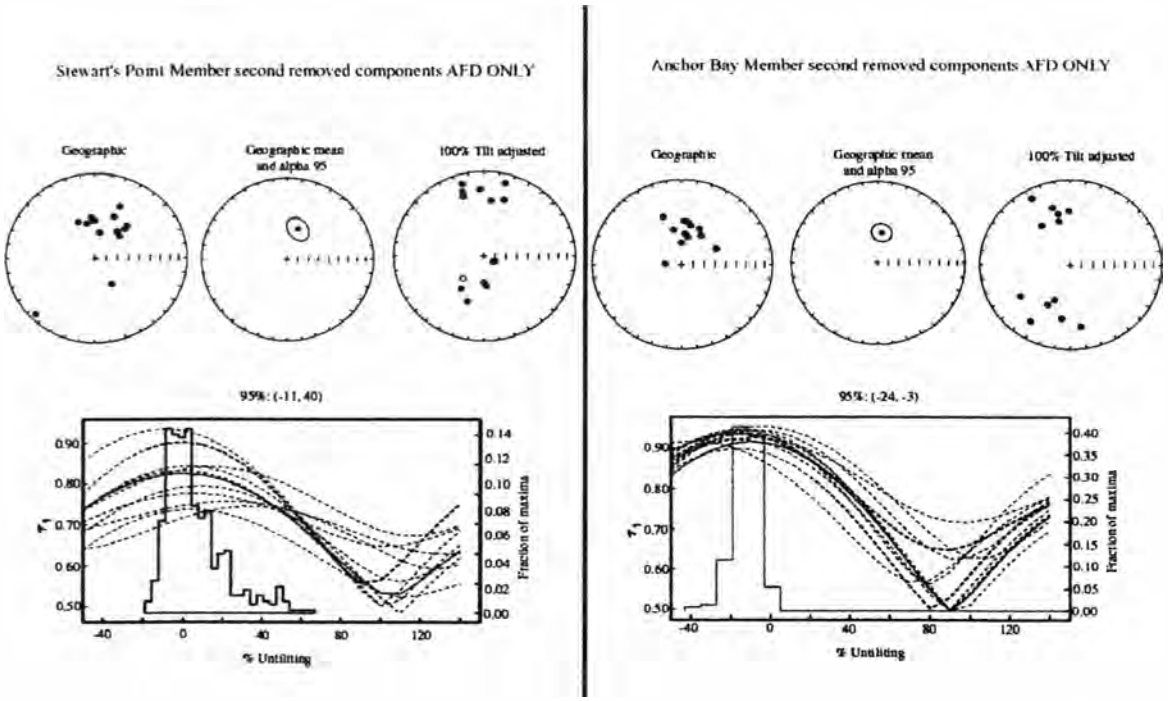

Figure 14. Equal area plots and fold test (Tauxe and Watson, 1994) of AFD only data. Solid line is the unfolding curve of the data. Dashed lines indicate unfolding of generated bootstrap data.

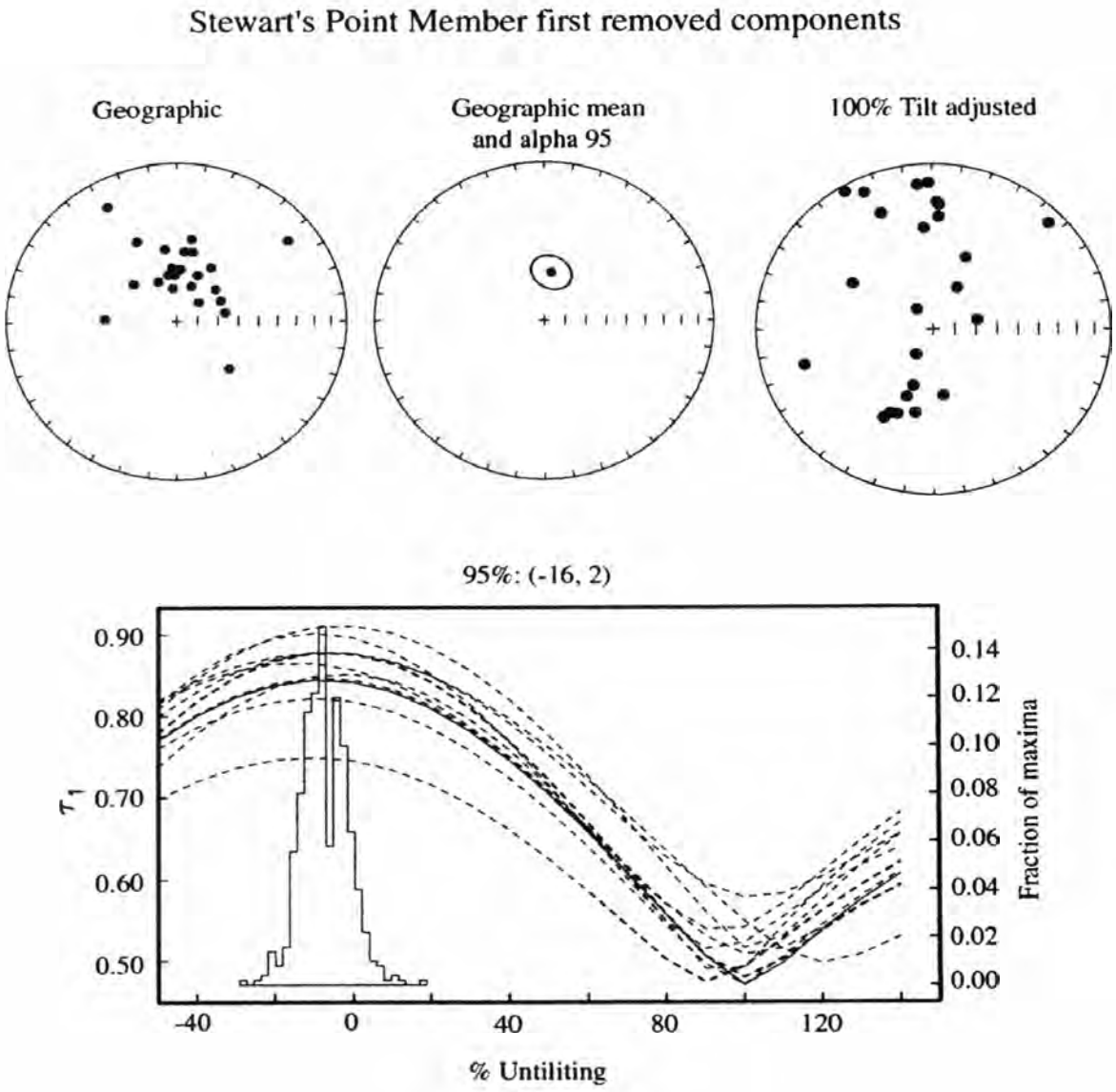

Figure 15. Equal area projections and fold test data for the first removed components from the Stewart's Point specimens. Fold test using first removed components from all demagnetization methods employed. Equal area plots show increased dispersion in stratigraphic coordinates. Solid line is the unfolding curve of the data. Dashed lines are iterations of generated bootstrap data. Minimum dispersion of directions occurs at ~7% unfolding.

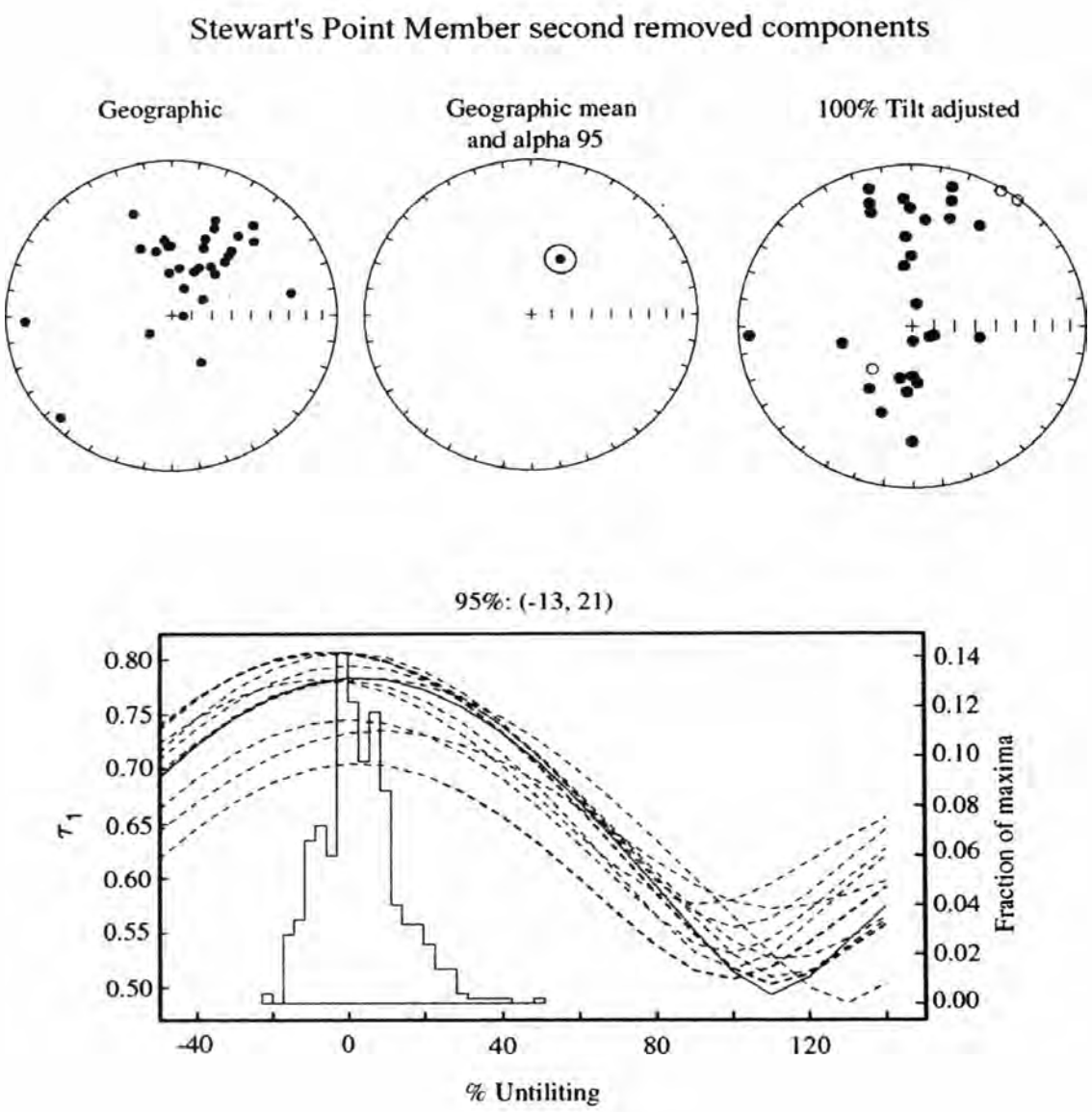

Figure 16. Equal area projections and fold test data for the second removed directions from the Stewart's Point specimens. Fold test using second removed components from all demagnetization methods employed. Equal area plots show increased dispersion in stratigraphic coordinates. Solid line is the unfolding curve of the data. Dashed lines indicate iterations of generated bootstrap data. Minimum dispersion of directions occurs at 0% unfolding.

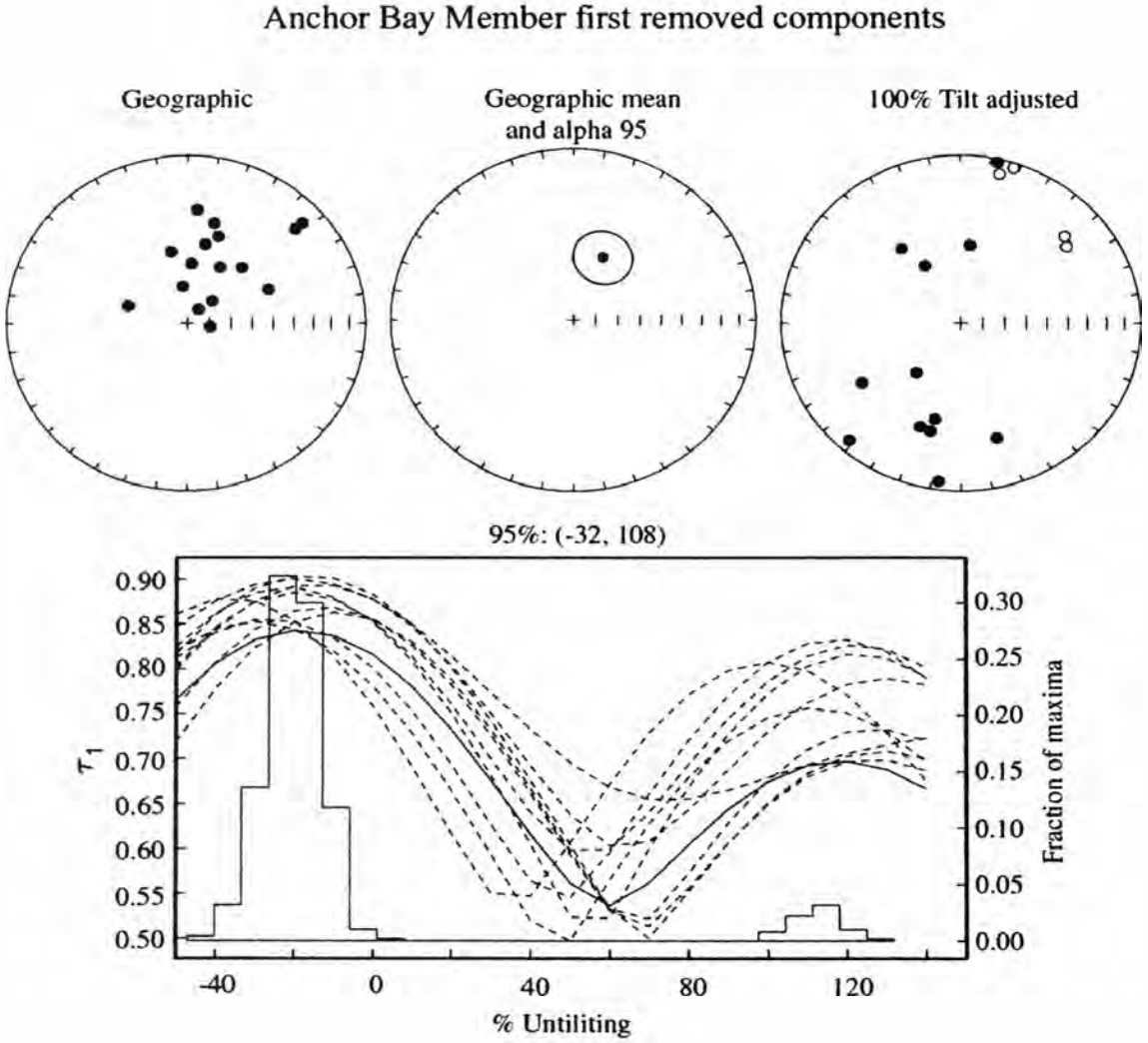

Figure 17. Equal area projections and fold test data for the first removed directions from the Anchor Bay specimens. Fold test using first removed components from all demagnetization methods employed. Equal area plots show increased dispersion in stratigraphic coordinates. Solid line is the unfolding curve of the data. Dashed lines indicate iterations of generated bootstrap data. Minimum dispersion of directions occurs at ~20% unfolding.

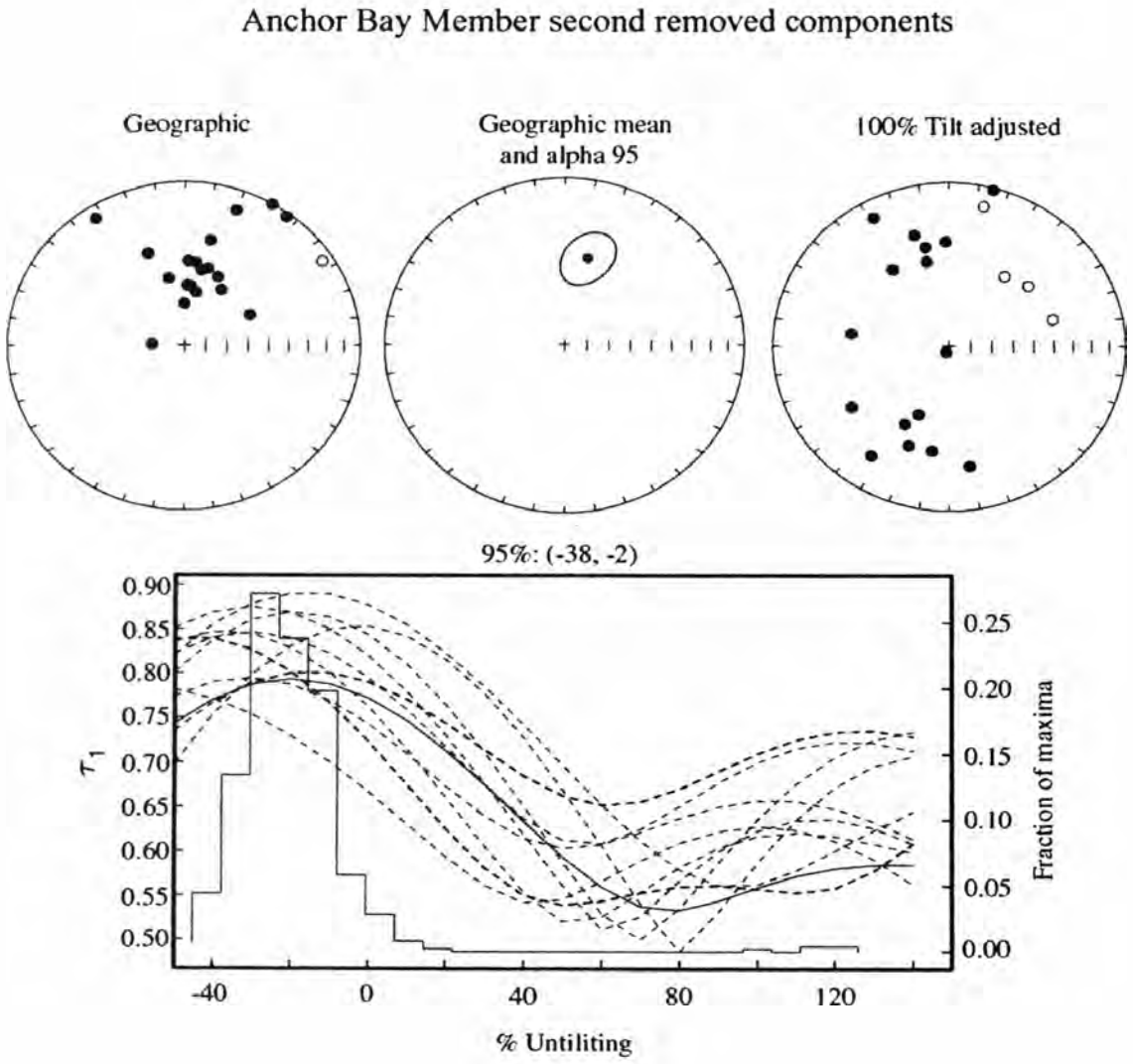

Figure 18. Equal area projections and fold test data for the second removed directions from the Anchor Bay specimens. Fold test using second removed components from all demagnetization methods employed. Equal area plots show increased dispersion in stratigraphic coordinates. Solid line is the unfolding curve of the data. Dashed lines indicate iterations of generated bootstrap data. Minimum dispersion of directions occurs at ~25% unfolding.

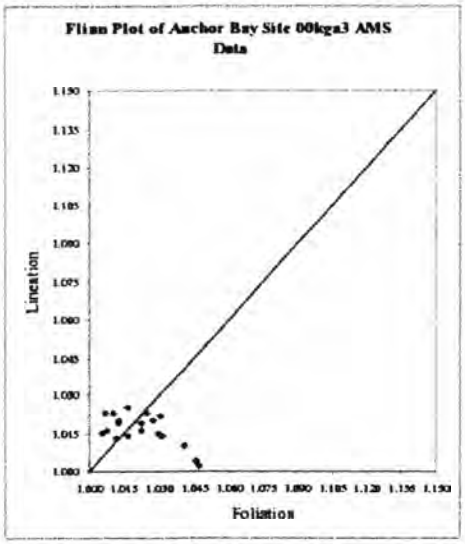

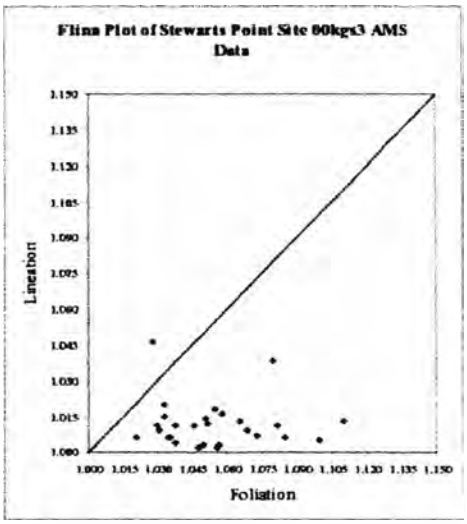

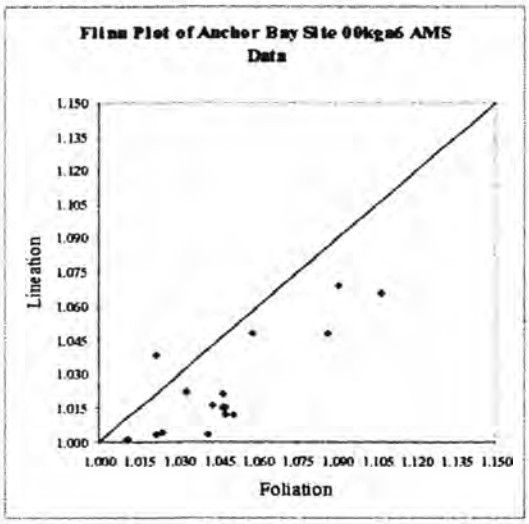

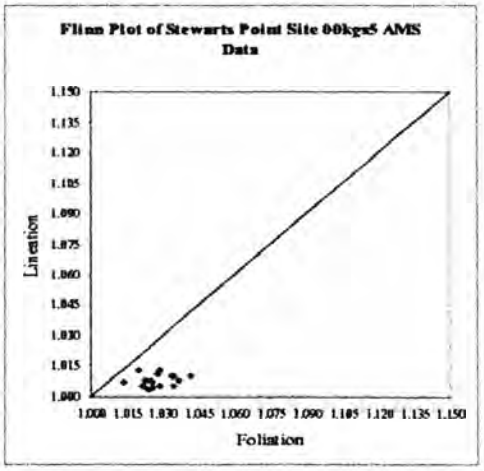

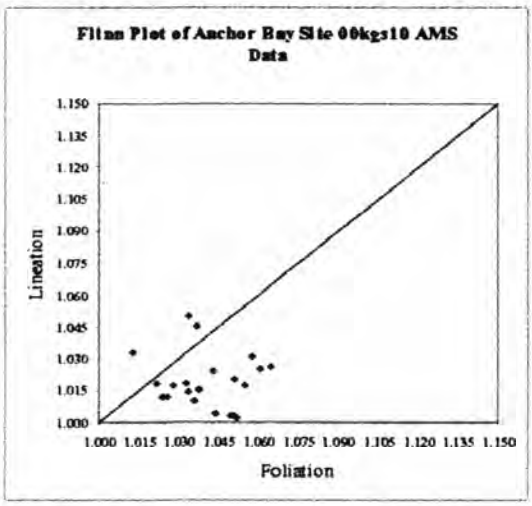

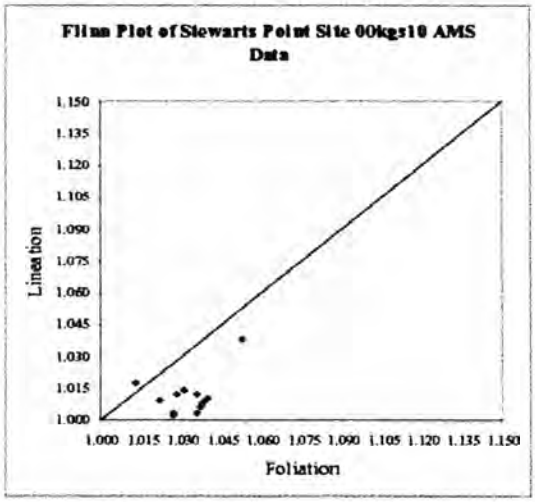

Figure 19. Flinn (1962) plots of shape parameters from AMS data. Lineation is plotted against foliation to determine the ellipsoid shapes. Upper left plot shows that fabric for Anchor Bay site 3 is triaxial; all other sites are dominated by oblate ellipsoid shapes or foliation-dominated.

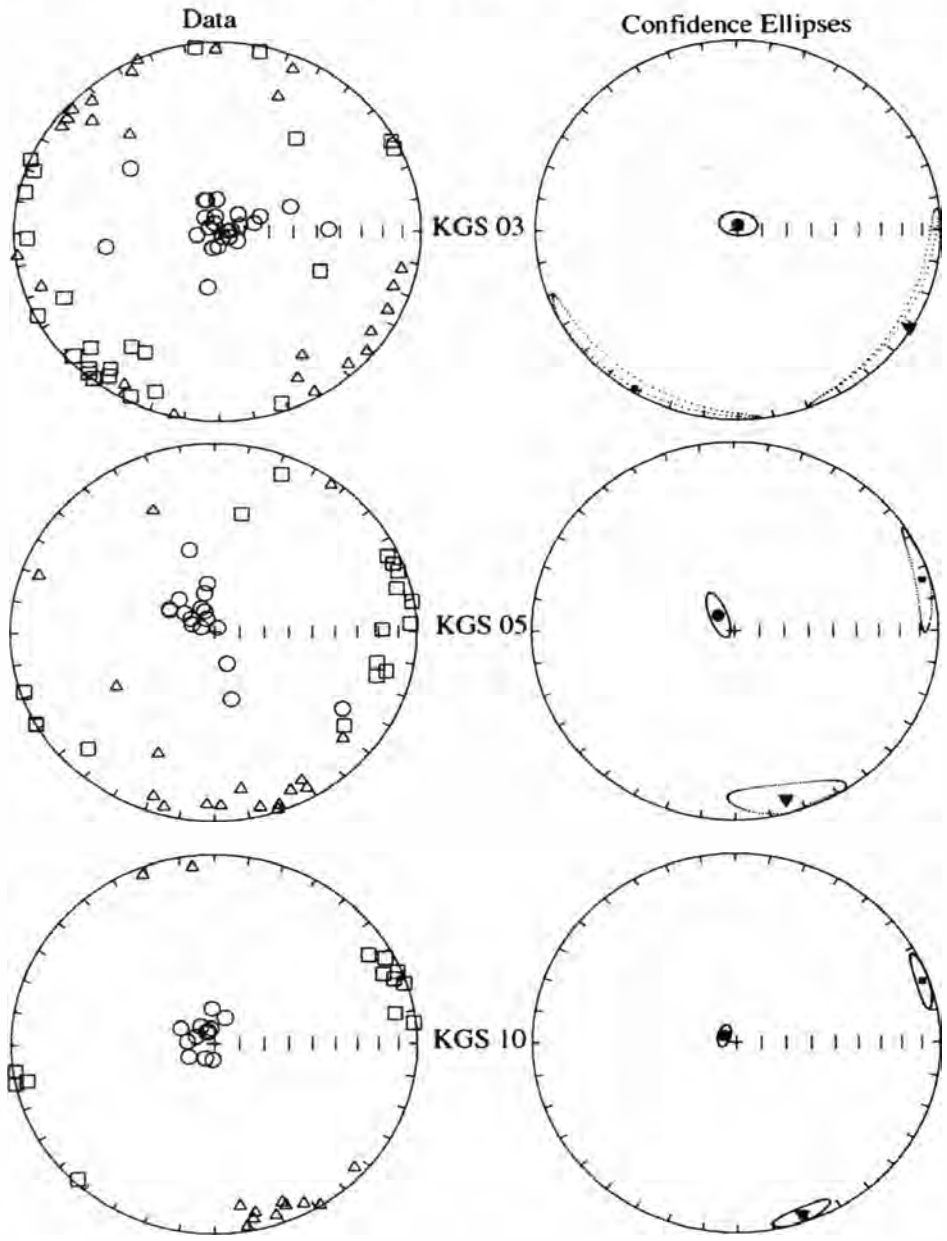

20a.

Figure 20a and 20b. Anisotropy of magnetic susceptibility equal area plots. Selected Stewart's Point member sites (a) and Anchor Bay member sites (b) in stratigraphic coordinates. Circles denote k-min, triangles k-int and squares k-max. k-min is nearly vertical.

Anchor Bay Anisotropy of Magnetic Susceptibility Plots

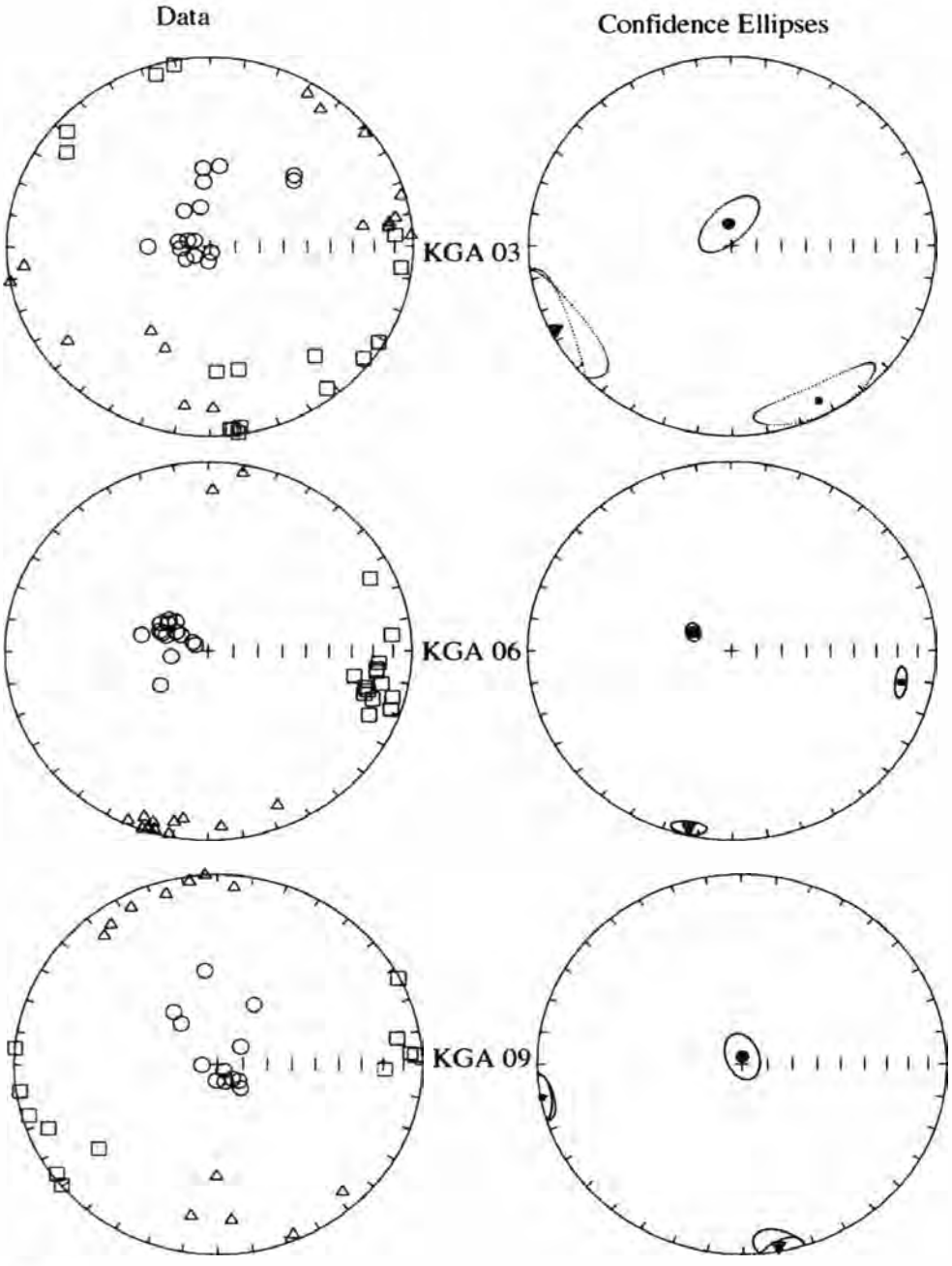

20b

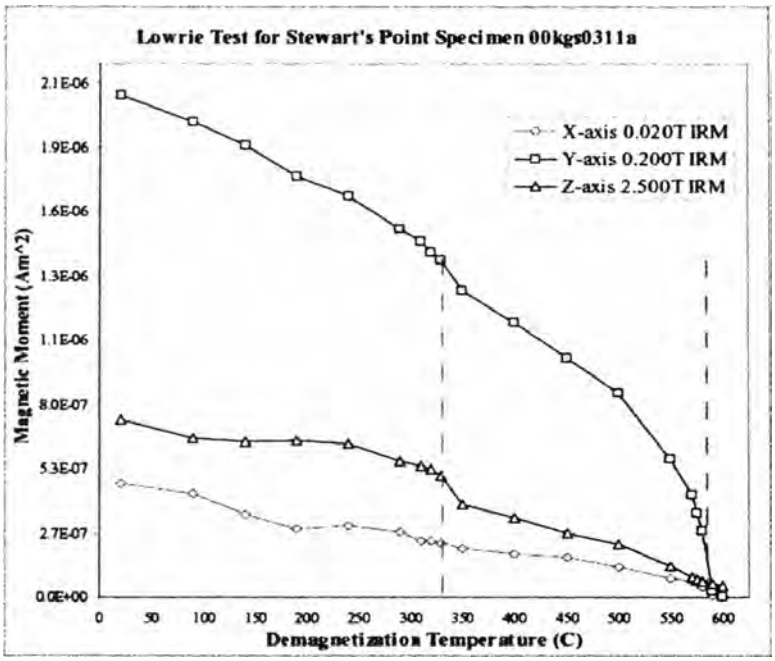

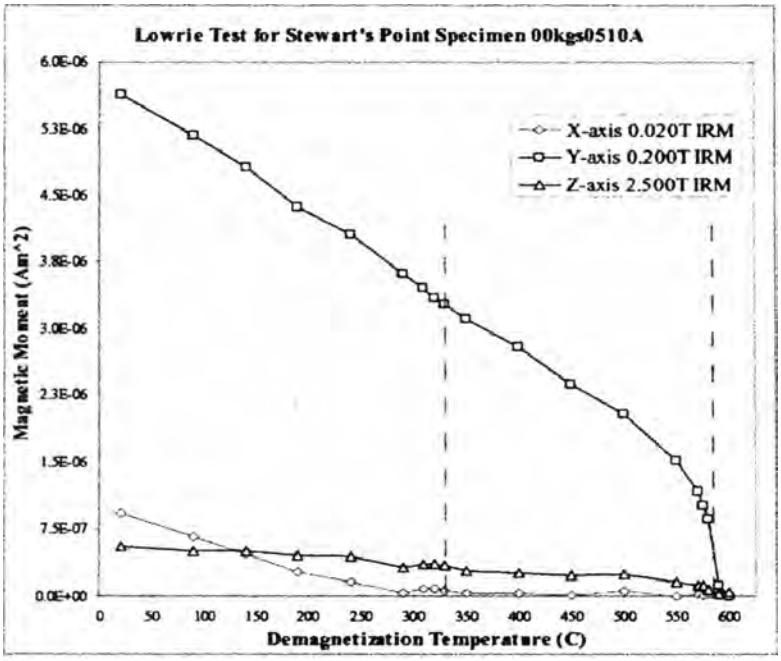

21a.

Figure 21a and 21b. Lowrie (1991) mIRM plots for selected Stewart's Point specimens (a) and Anchor Bay specimens (b). Dashed gray lines indicate the Curie temperatures for pyrrhotite at 320 °C and magnetite at 580°C. All specimens show a drop in magnetization at 580°C and a few, like 00KGS311a, show a drop at 320° C.

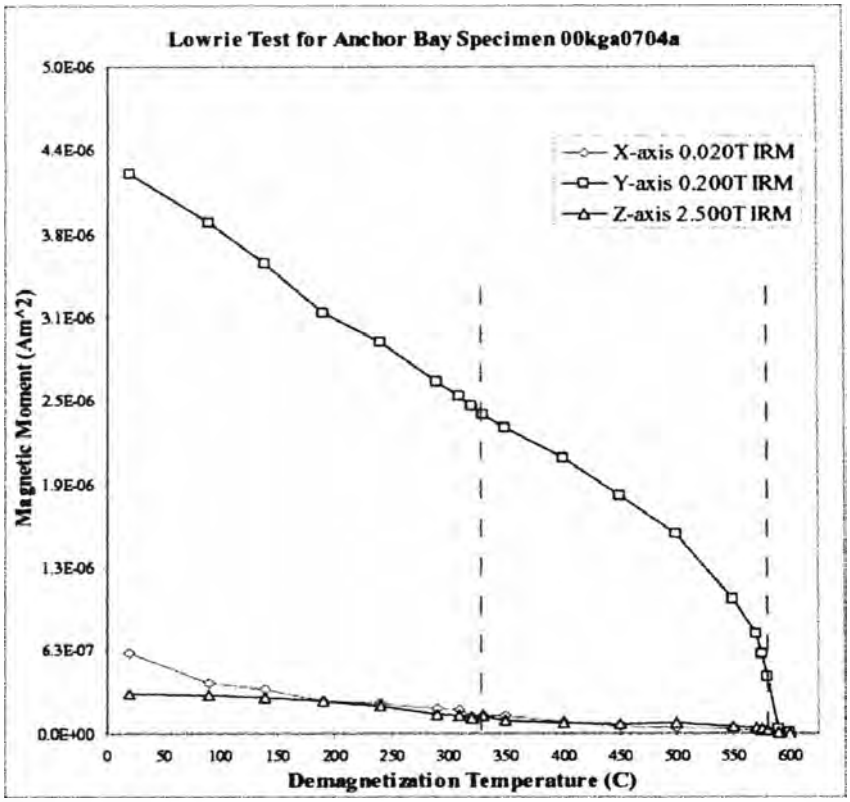
Lowrie Test for Anchor Bay Specimen 00kga0704a
X-axis 0.020T IRM
Y-axis 0.200T IRM
Z-axis 2.500T IRM
Magnetic Moment (Am^2)
5.0E-06
4.4E-06
3.8E-06
3.1E-06
2.5E-06
1.9E-06
1.3E-06
6.3E-07
0.0E+00
0
50
100
150
200
250
300
350
400
450
500
550
600
Demagnetization Temperature (C)

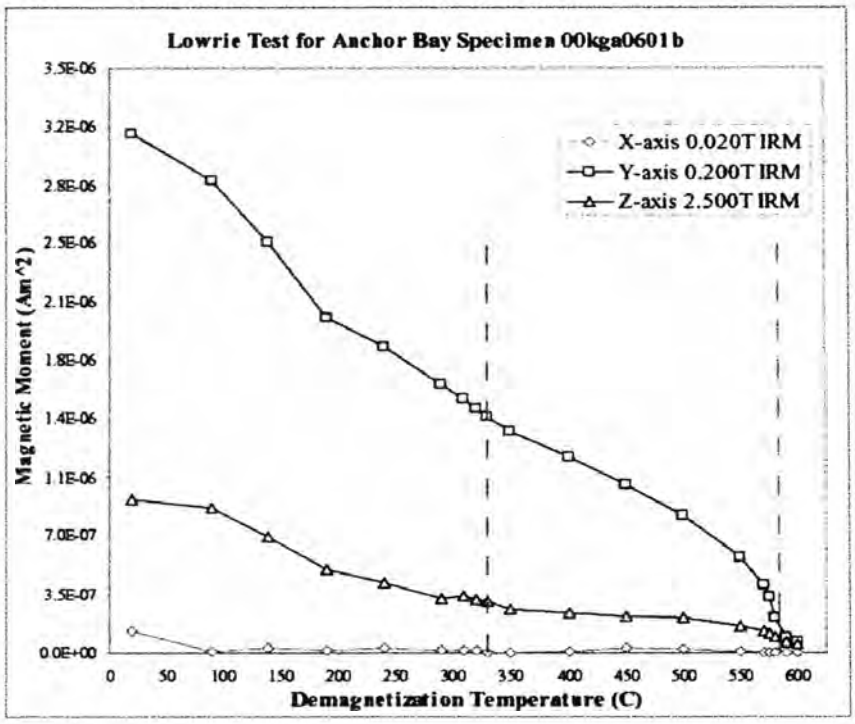
Lowrie Test for Anchor Bay Specimen 00kga0601b
X-axis 0.020T IRM
Y-axis 0.200T IRM
Z-axis 2.500T IRM
Magnetic Moment (Am^2)
3.5E-06
3.2E-06
2.8E-06
2.5E-06
2.1E-06
1.8E-06
1.4E-06
1.1E-06
7.0E-07
3.5E-07
0.0E+00
0
50
100
150
200
250
300
350
400
450
500
550
600
Demagnetization Temperature (C)

21b.

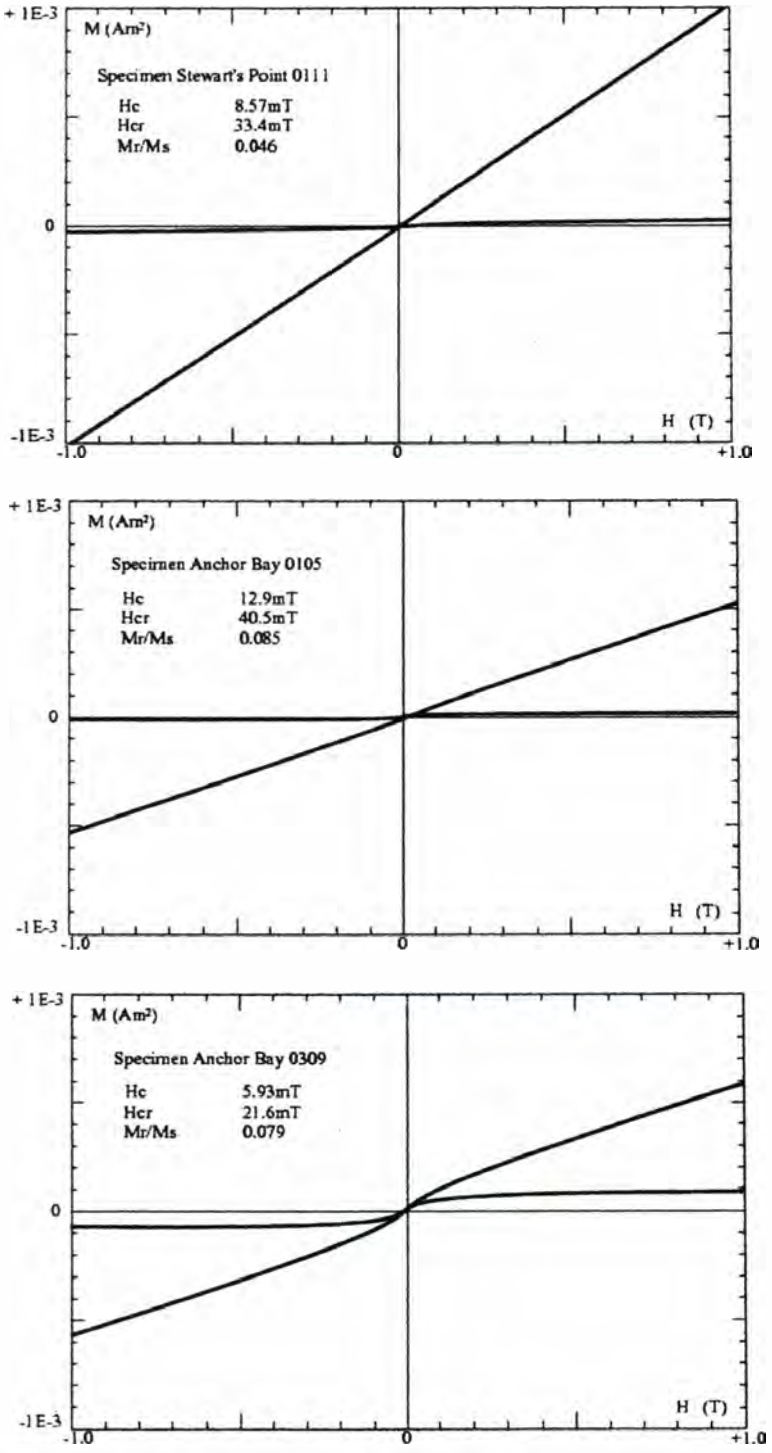

Figure 22. Hysteresis plots for Stewart's Point and Anchor Bay specimens: top specimen is nearly superparamagnetic, middle and bottom specimens are wasp-waisted, pseudo-single domain. Axes represent the applied field (x-axis) and the magnetic moment (y-axis).

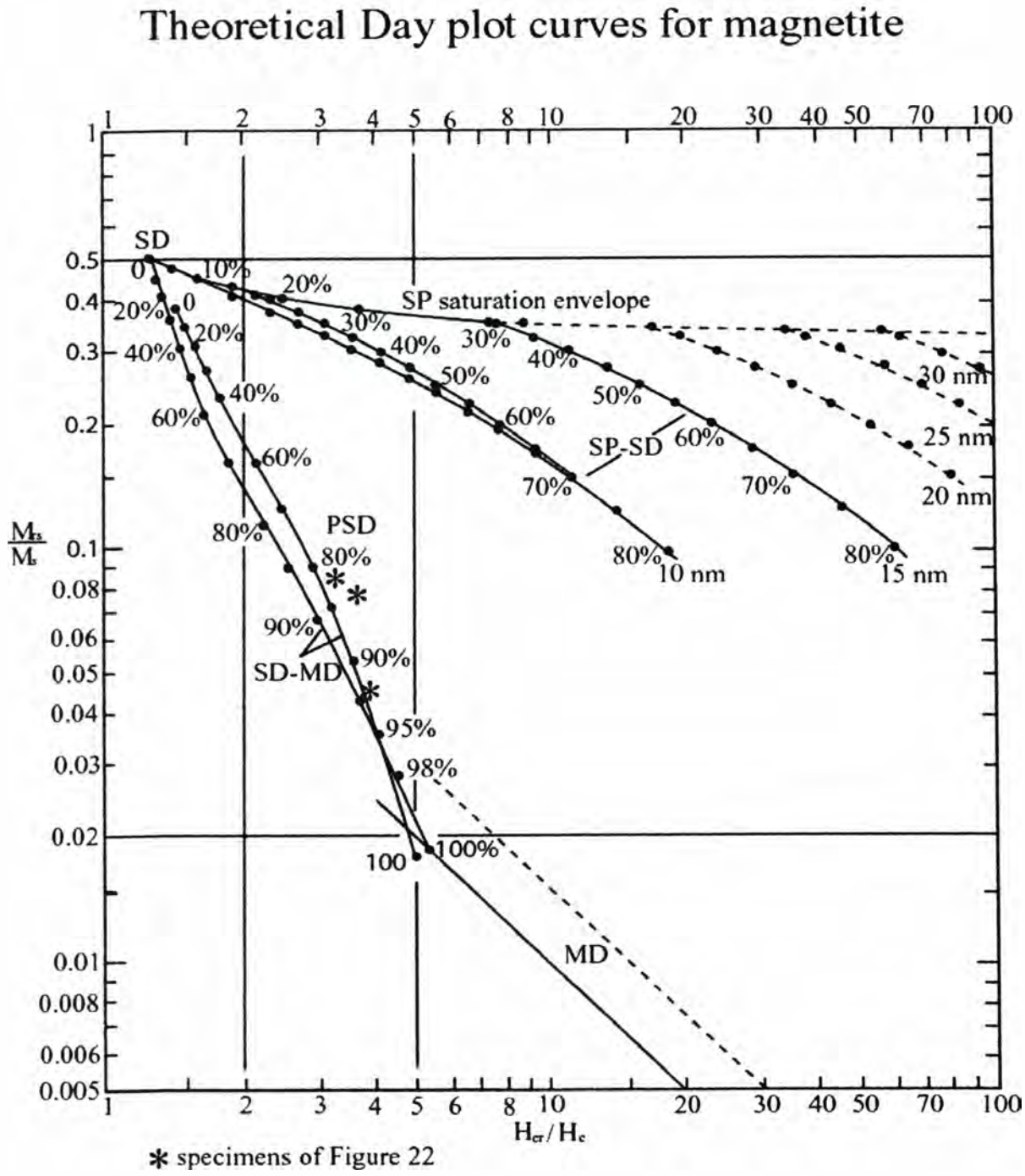

Figure 23. Modified Day plot for magnetite after Dunlop (2002). Red asterisks denote specimens with hysteresis data from Figure 22. Specimens plot in Pseudo-single domain range near the mixing curves for single domain and multi-domain magnetites.

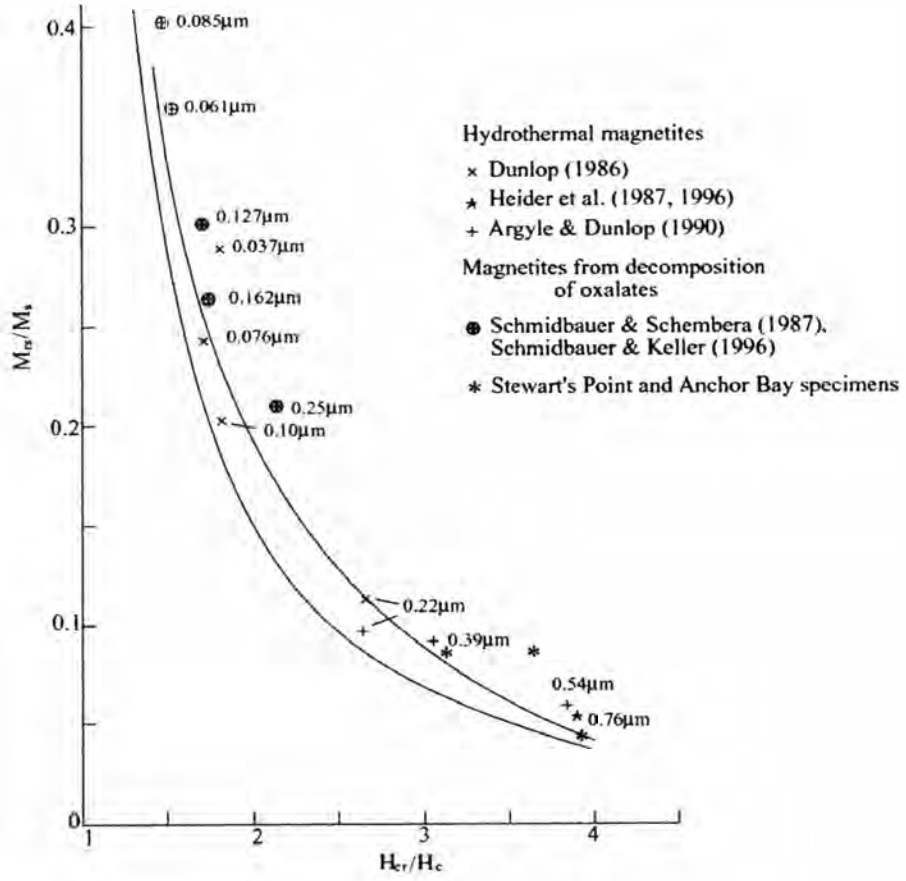

Figure 24. Modified Day plot after Dunlop (2002) showing mixing curves for single domain and multi-domain magnetite with sized magnitites plotted. Red asterisks denote specimens with hysteresis data from Figure 22. Specimens plot in range of .22 to .76 μm.

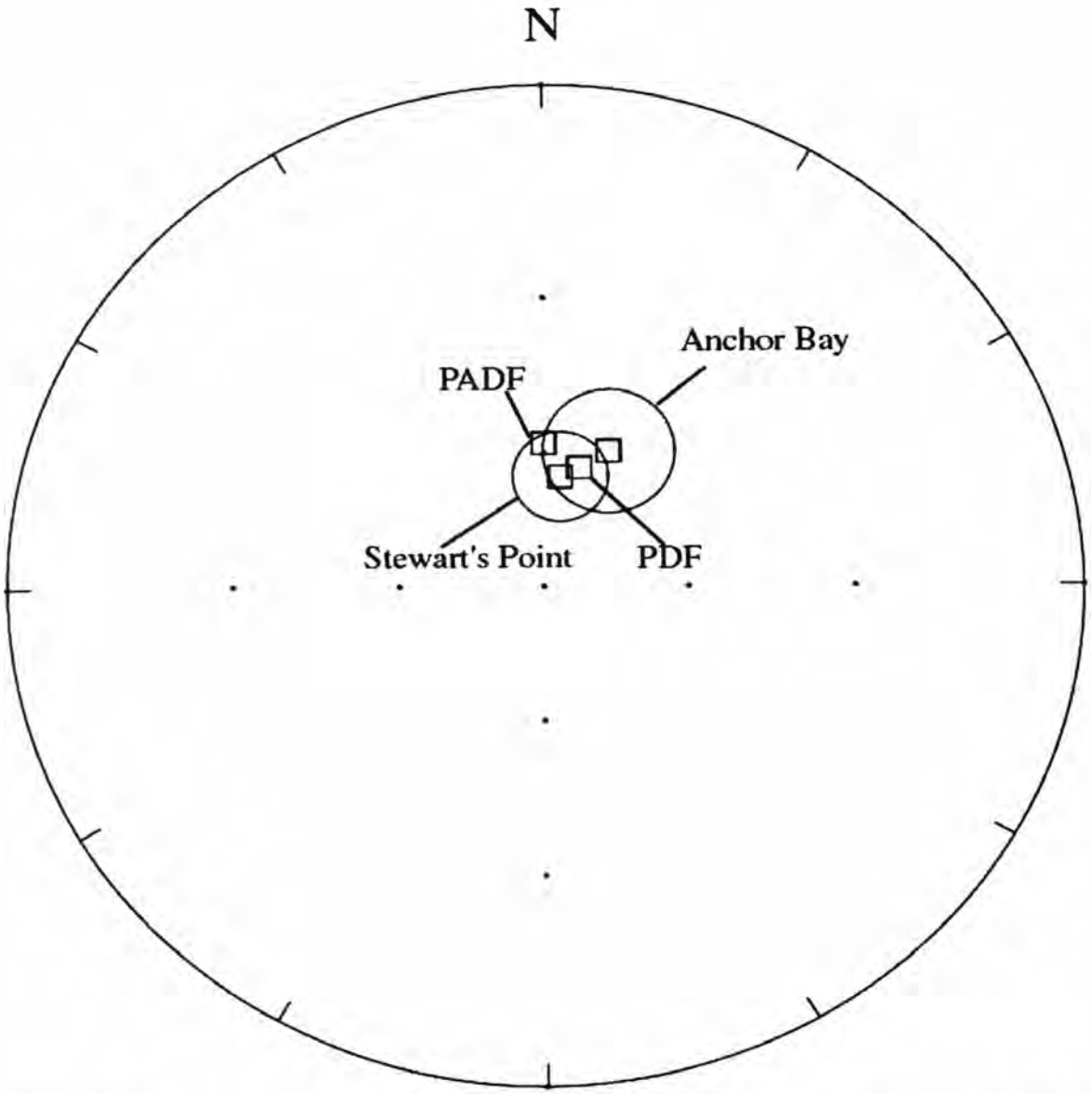

Figure 25. Equal area projection of first removed components from Stewart's Point and Anchor Bay members with corresponding 95% circles of confidence. Present day field (PDF) and present day axial dipole field (PADF) are within the circles of confidence for the means.

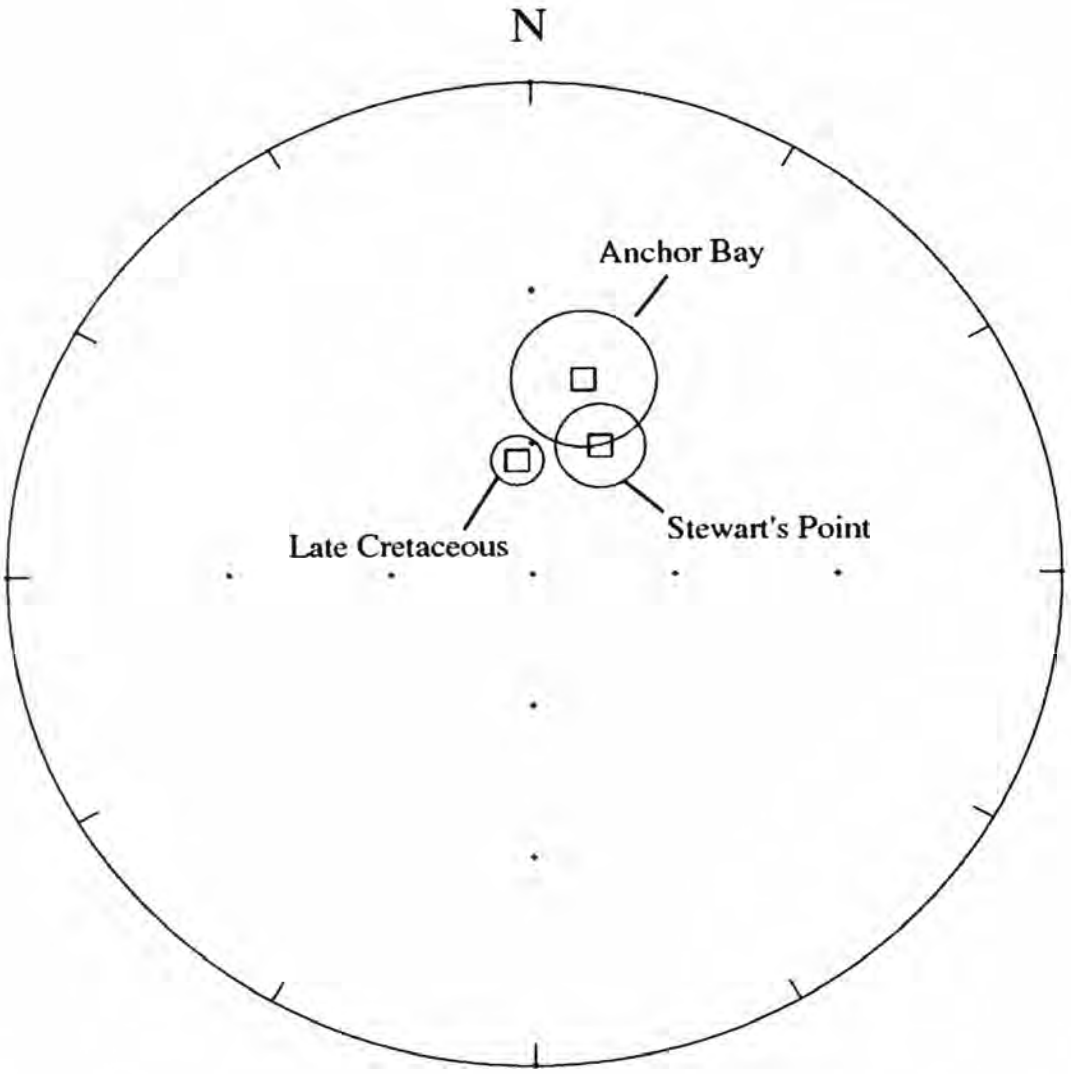

Figure 26. Equal area projection of second removed components from Stewart's Point and Anchor Bay members with the Late Cretaceous calculated direction for the Point Arena terrane (from Diehl, 1991; Gunderson and Sheriff, 1991).

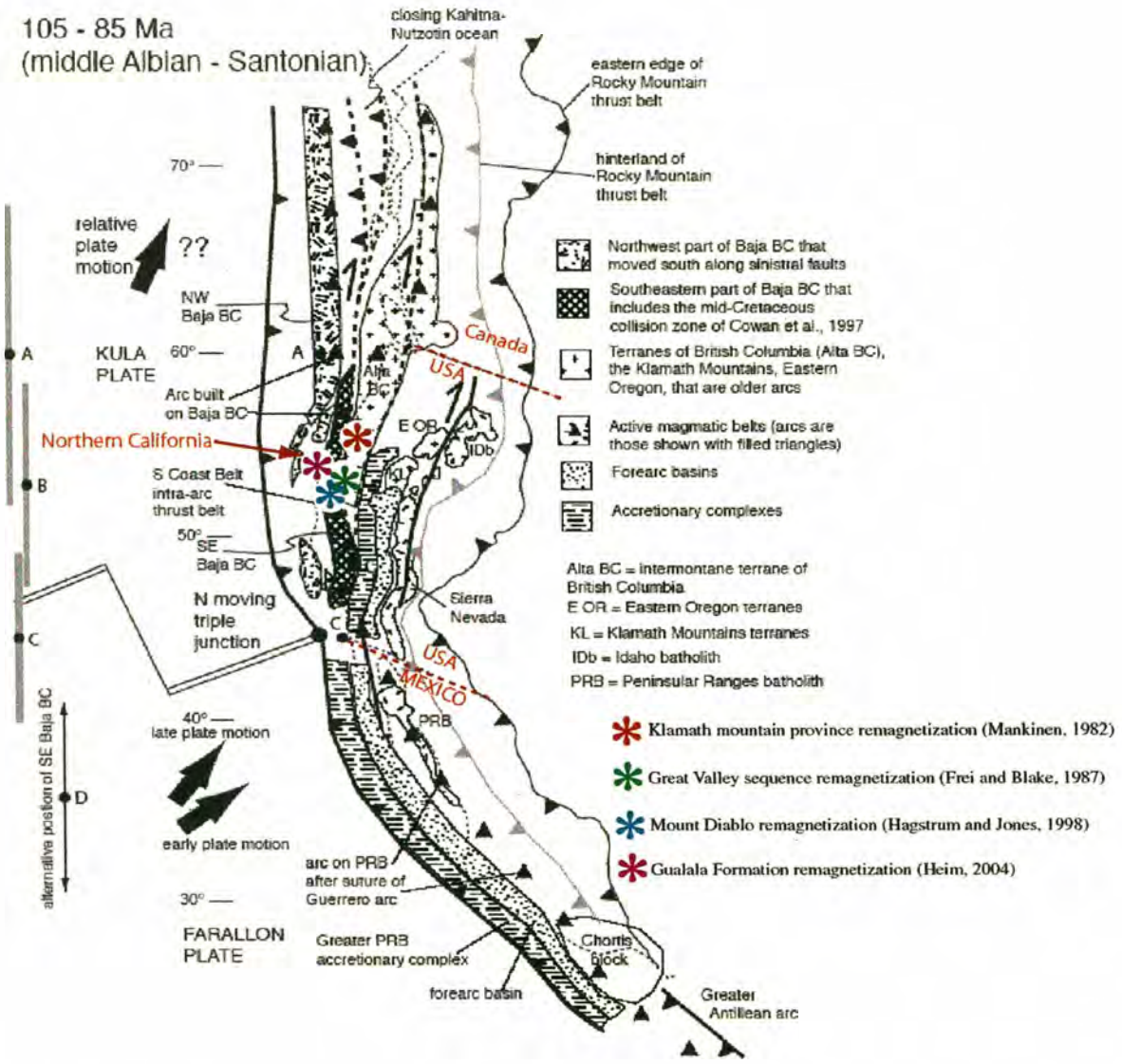

Figure 27. Late Cretaceous reconstruction of the western margin of North America (modified from Umhoeffer, 2002). Upper Cretaceous sediments showing remagnetization (Mankinen, 1982; Frei and Blake, 1987; Hagstrum and Jones, 1998) and this study are indicated.

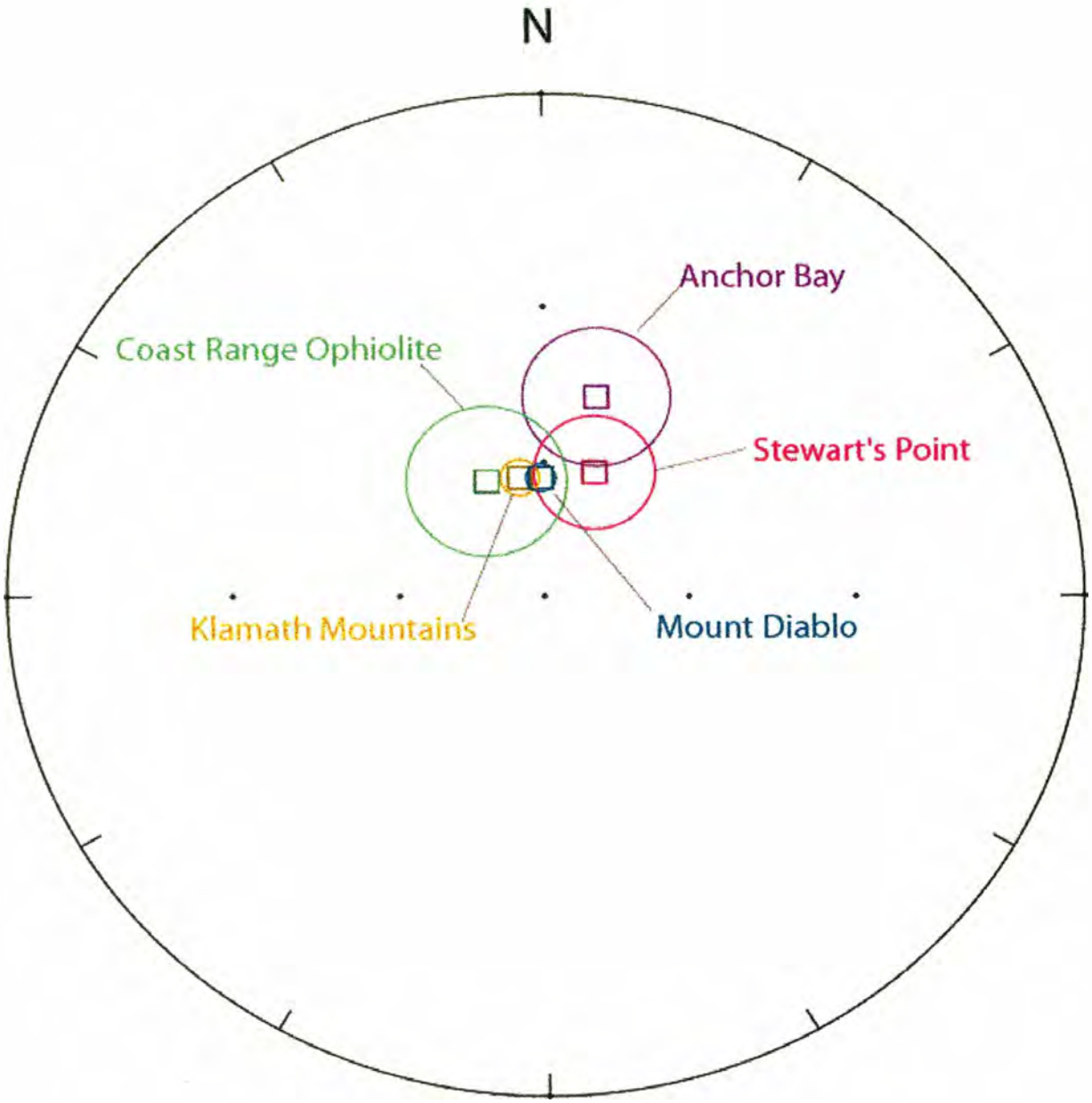

Figure 28. Comparison of remagnetization studies of Mount Diablo (Hagstrum and Jones, 1998), the Klamath mountains (Mankinen, 1982) and the Coast Range ophiolite (Frei and Blake, 1998) with results from the Stewart's Point and Anchor Bay members of the Gualala Formation.

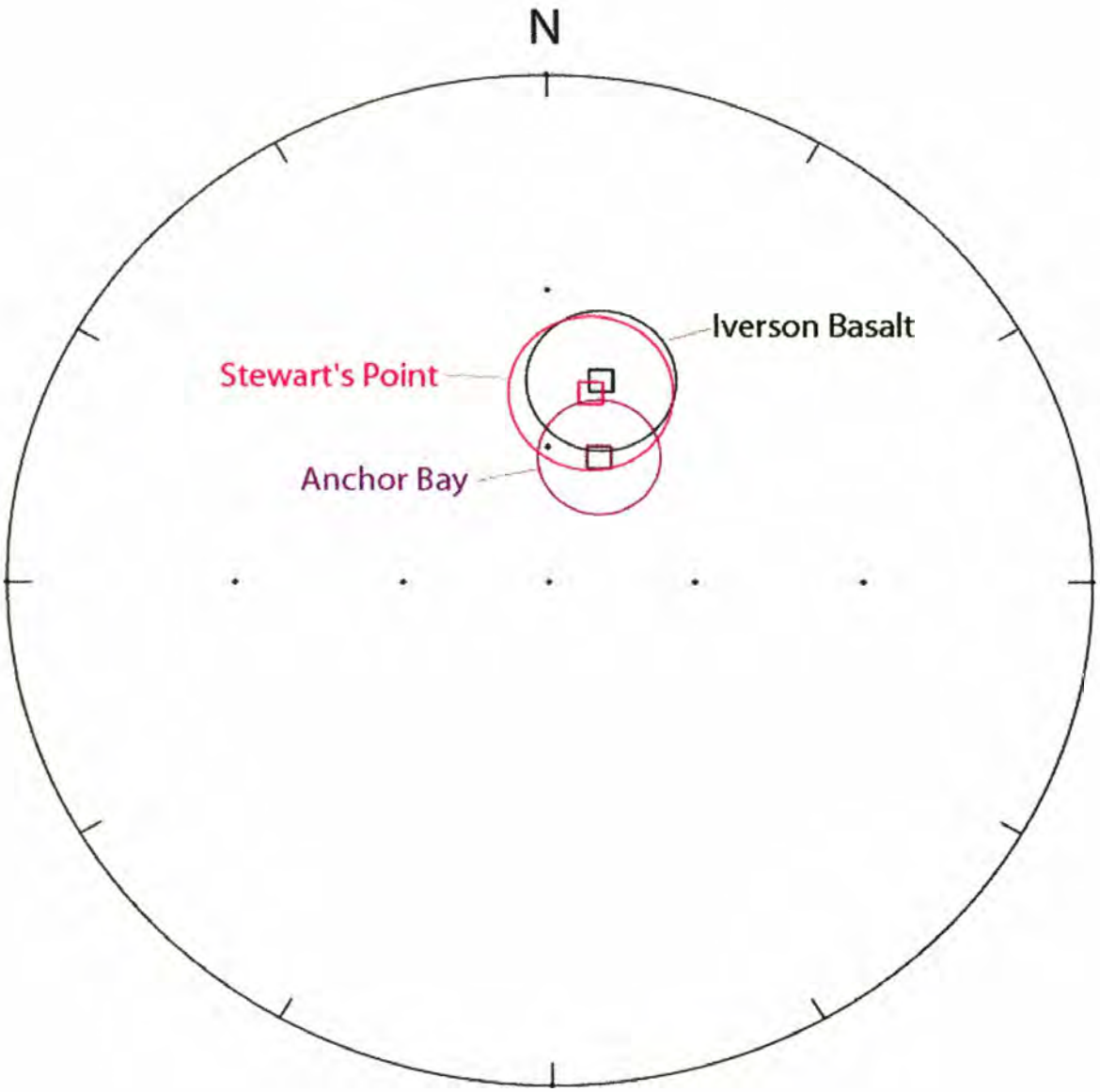

Figure 29. Comparison of Iverson Basalt direction (inverted) with Stewart's Point and Anchor Bay members of the Gualala Formation.

	First removed component			Second removed component		
Member	declination	inclination	alpha95	declination	inclination	alpha95
Stewart's Point	8.0	64.9	9.7	26.3	57.4	8.9
Anchor Bay	24.1	57.0	12.9	13.9	45.5	13.4
Stewart's Point (AFD only)				18.2	57.7	11.8
Anchor Bay (AFD only)				7.7	59.0	10.0
Present day magnetic field	15.7	62.2				
Present day axial dipole field	0.0	58.0				
Late Cretaceous magnetic field	353.2	63.6	5.4			

Table 1. Summary of Paleomagnetic Data from the Stewart's Point and Anchor Bay members of the Gualala Formation with North American reference poles for present day and the Late Cretaceous. Late Cretaceous direction is calculated for study location from the average of Diehl (1991) and Gunderson and Sheriff (1991) paleopoles.